THE DEVELOPMENT OF POTENTIAL THERAPEUTIC ANTI-MYOSIN S2 PEPTIDES THAT MODULATE CONTRACTION AND APPEND TO THE HEART HOMING ADDUCT TANNIC ACID WITHOUT NOTICEABLE EFFECT ON THEIR FUNCTIONS

Motamed MKH A Qadan, M.S.

Dissertation Prepared for the Degree of

DOCTOR OF PHILOSOPHY

UNIVERSITY OF NORTH TEXAS

May 2021

APPROVED:

Douglas D. Root, Major Professor
Pamela A. Padilla, Committee Member
Pudur Jagadeeswaran, Committee Member
Robert C. Benjamin, Committee Member
Xiaoqiang Wang, Committee Member
Jyoti Shah, Chair of the Department of Biological Sciences
Su Gao, Dean of the College of Science
Victor Prybutok, Dean of the Toulouse Graduate School

Qadan, Motamed MKH A. *The Development of Potential Therapeutic Anti-Myosin S2 Peptides that Modulate Contraction and Append to the Heart Homing Adduct Tannic Acid without Noticeable Effect on Their Functions*. Doctor of Philosophy (Biochemistry and Molecular Biology), May 2021, 76 pp., 5 tables, 25 figures, references, 105 titles.

This dissertation aimed to explore the S2 region with an attempt to modulate its elasticity in order to tune the contraction output. Two peptides, the stabilizer and destabilizer, showed high potential in modifying the S2 region at the cellular level, thus they were prepared for animal model testing. In this research, (i) S2 elasticity was studied, and the stabilizer and destabilizer peptides were built to tune contraction output through modulating S2 flexibility; (ii) the peptides were attached to heart homing adducts and the bond between them was confirmed; and (iii) it was shown that minor changes were imposed on the modulating peptides' functionality upon attaching to the heart homing adducts.

S2 flexibility was confirmed through comparing it to other parts of myosin using simulated force spectroscopy. Modulatory peptides were built and computationally tested for their efficacy through interaction energy measurement, simulated force spectroscopy and molecular dynamics; these were attached to heart homing adducts for heart delivery. Interaction energy tests determined that tannic acid (TA) served well for this purpose. The stoichiometry of the bond between the TA and the modulating peptides was confirmed using mass spectroscopy. The functionality of the modulating peptides was shown to be unaltered through expansion microscopy where they located to the same position on the sarcomere with and without TA. They were also shown to cause the sarcomeres to contract similarly with and without the TA in contractility assay. Taken together, this work prepared the modulating peptides for animal model tests by attaching them to tannic acid.

ACKNOWLEDGMENTS

First and foremost, all thanks belong to God. Then, my deepest gratitude and respect to Dr Root for his patience with my nonsensical mistakes, for his guidance and dedication and for his endless knowledge. I also hold very special appreciation for Dr Wang for teaching me the basics of crystallography. I am no less grateful to Dr Padilla and Dr Benjamin for expanding my knowledge through their classes, and to Dr Jag for his mind-triggering questions. Many thanks to Dr Andrea for being a wonderful caring person, and to Dr Verbeck for opening his lab to run the mass spec experiments. Special thanks to his student Rachel who always welcomed me with a smile and bore with running the experiments. I am also very thankful to the lab members whom I built a life-long relation: Duaa, Rohit, Negar and Julia. Special thanks to Kim for her spirit and pleasant replies and to Arland who has been one of the best easy-going TA supervisors. Thanks to Heather who always has been very helpful. Special thanks for two professors from my previous degrees Dr Bdour and Dr Laufer for being highly dedicated towards teaching. I would like also to extend many thanks to Dr Masri and Dr Pedersen in particular for sending several recommendations and for providing me with my first lab experience. Very Special thanks both to my close uncle who generously offered me financial support and has always been a great source of help, and to my in-laws who have always been caring, passionate and immensely supportive in all our steps. I would like to send dedicated thanks to my brothers who are true blessings: Dr Maen who has been my role model and sheltered me for 2.5 years providing all the support and guidance. Mutaz who supported me a lot financially and cared for me, something that I will never forget for both. Motasem for being the supportive younger brother that I will always care for. Two of the most

heartful thanks are: to my wife for making everything much more enjoyable after it was tasteless before, and for being my family and home abroad. And to my parents, who among all people, will never be able to payback for supporting me and feeling with me like no other. No words can express my gratitude. Lasty, I am closing this chapter of my life with lifelong engraved memories from Texas, a Ph.D degree and best of all a family that is a true grace.

TABLE OF CONTENTS

Page

LIST OF TABLES

Page

LIST OF FIGURES

Page

ABBREVIATIONS

Φ	Phi
Ψ	Psi
A^{o}	Angstrom
A band	Anisotropic band
ADP	Adenosine di phosphate
ATP	Adenosine tri phosphate
APS	Ammonium Persulfate
BCA	Bicinchoninic acid assay
Bis-tris	bis(2-hydroxyethyl)iminotris(hydroxymethyl)methane
^{o}C	Celcius
C18	18 Carbons matrix column
Ca^{+2}	Calcium
CaCl2	Calcium Chloride
C-end	Carboxylic end of protein
CPP	Cell penetrating peptides
Cu+1	Cupper
DCM	Dilated cardiomyopathy
DE	Destabilizer
-∫ dH/∫ dx	Decrease in H-bonds over extension
DMF	Dimethylfluoride
DMSO	Dimethylsulfoxide
E930del	Glutamate 930 deletion
EDTA	Ethylenediaminetetraacetic acid
EF	Ejection fraction
ELC	Essential light chain
ELISA	Enzyme-linked immunosorbent assay
ESI	Electrospray ionization
F	Force at extension x
F actin	Filamentous actin
FHCM	Familial hypertrophic cardiomyopathy

FITC	Fluorescein isothiocyanate
G actin	Globular actin
GFP	Green fluorescent protein
HCL	Hydrochloride
HHP	Heart homing peptide
HIV	Human immune-deficiency virus
HMM	Heavy meromyosin
HR1	Heptad repeat domain 1
I band	Isotropic band
IEC	Ion exchange chromatography
K	Spring constant
kB	Boltzmann's constant
kJ	KiloJouls
LMM	Light meromyosin
M	Molar
MALDI-TOF	Matrix assisted laser desorption ionization-time of flight
Mg^{+2}	Magnesium
ml	Milliliter
µls	Microliters
M-line	Mittelscheibe (German) middle disk
mM	Millimolar
Myosin S1	Myosin sub-fragment 1
Myosin S2	Myosin sub-fragment 2
MyBPC	Myosin binding protein C
NaCl	Sodium chloride
NaOH	Sodium hydroxide
N-end	Amino terminus of protein
NIH	National Institute of Health
nm	Nanometer
ns	Nanosecond
P53	Tumor protein 53
PBS	Phosphate buffered sailne

PEVK domain	(Proline, gluµmate, valine and lysine) domain in titin
pH	Potential of Hydrogen
pN	PicoNewton
Quan-TOF	Quantitative-time of flight
RLC	Regulatory light chain
RPC	Reverse phase chromatography
SARS-CoV-2	Severe acute respiratory syndrome - Coronaviruse-2
SFS	Simulated force spectroscopy
SR	Sarcoplasmic reticulum
ST	Stabilizer
T	Temperature
TA	Tannic acid
TA-DE	Tannic acid-Destabilizer
TA-ST	Tannic acid-Stabilizer
TEMED	Tetramethylethylenediamine
TEMPO	2,2,6,6-Tetramethylpiperidin-1-yl)oxyl
TFA	Trifluoroacitic acid
Tmod	Tropomodulin
TRITC	Tetramethylrhodamine
Troponin I	Troponin inhibitory domain
Troponin C	Troponin calcium domain
Troponin T	Troponin tropomodulin domain
V	Proportionality constant in units of distance−1
WT	Wild type
X	The difference between the intended and the actual separation
Z-line	Zwischenscheibe (German) spacer

CHAPTER 1

INTRODUCTION

1.1 Muscles

Muscle contraction is one of the fascinating cellular activities that can be observed under the microscope. The organized pattern of striated muscle cells further adds to this charming experience. All three types of muscles including skeletal, smooth, and cardiac muscle cells are thought to undergo contraction according to the sliding filament theory. In this theory myosin reaches to actin after hydrolyzing an ATP molecule, it then undergoes conformational change upon the release of the hydrolyzed ATP (ADP-Pi) in what is known as the “power stroke” leading to a 45-90^{o} bend in the myosin head (Al Khayat, 2013), which causes the actin to be pulled towards the M line producing a contraction. The myosin heads are released from actin upon binding another ATP molecule to start another contraction cycle. Calcium is a pivotal element in this process, it influxes inside the cell upon stimulation and binds to ryanodine receptors on the sarcoplasmic reticulum (SR) causing their gates to open and release more calcium (Hong and Shaw, 2017; Betts et al., 2013) which causes the inhibitory proteins to be released from actin (see below), thus allowing contraction to occur.

Different muscle types have different properties and different functions: skeletal muscle cells are striated and have well-defined repeated structures called sarcomeres. These are considered the contractile units in the cells and are bordered by two z disks (Fig. 1.1). They are multinucleated and completely depend on neuronal activation for contraction. The number of myofibers (muscle cells) in the muscle do not change, but the sarcomeres and the myofibril increase or decrease in size (Betts et al., 2013).

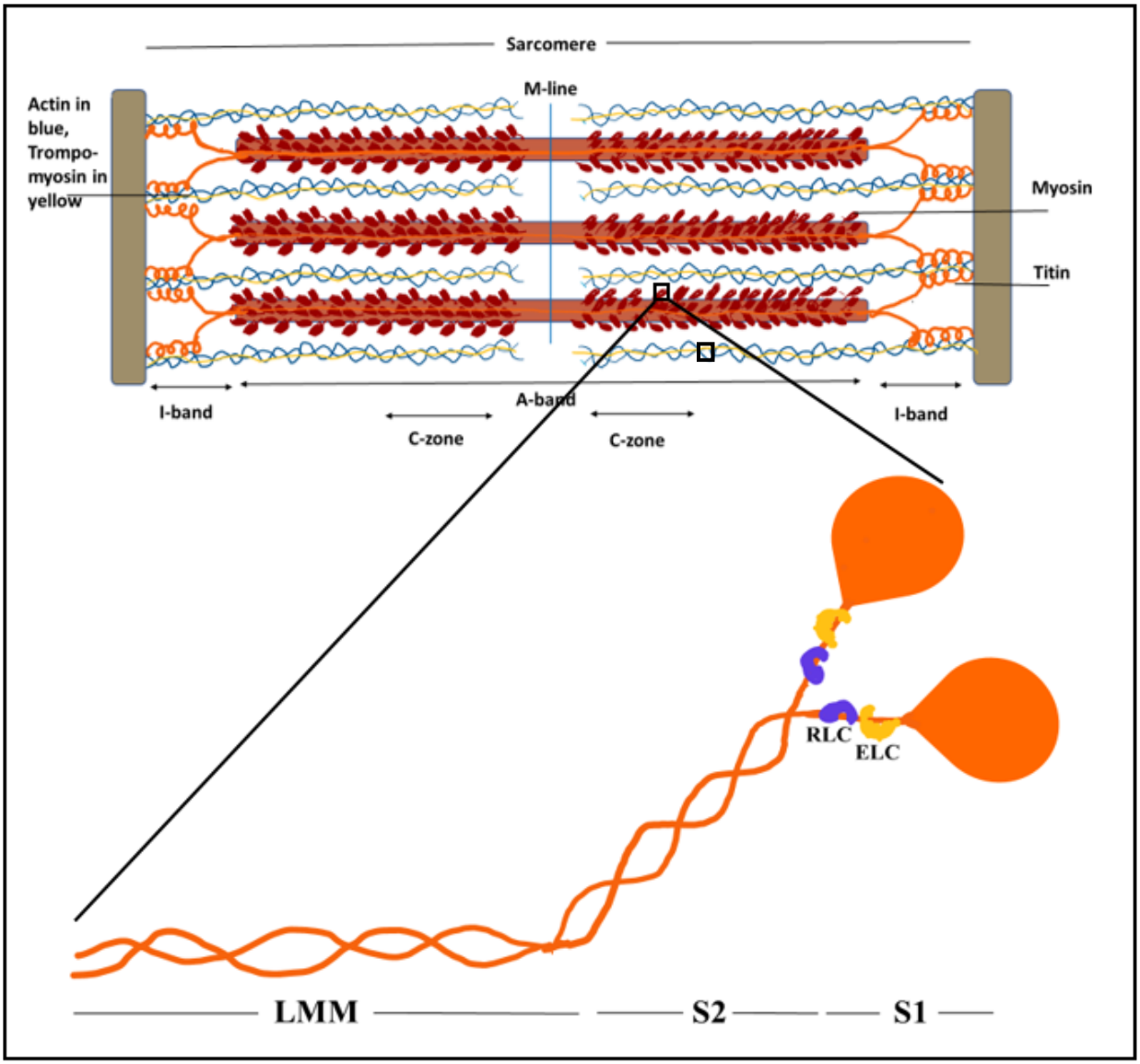

Figure 1.1: A Sarcomere of a typical striated muscle and an enlarged illustration for a myosin molecule. The image on the top is an illustration for some of the major proteins and bands in the sarcomere. The actual number of different protein types in the muscle sarcomere is much higher. The image in the bottom is an enlargement for the myosin molecule showing the major structural divisions S1, S2 and LMM.

Smooth muscle cells, on the other hand, are special in that they lack sarcomeres. They are almost thousand times shorter than skeletal muscle cells and have a single nucleus in their cytoplasm. They are spindle shaped cells; wide in the middle and tapered at the ends. Unlike skeletal muscles however, their contraction is involuntary and may involve the nervous system, but can also be controlled by other pathways such as

hormones or physical stimuli that eventually lead to opening of the calcium channels on the sarcolemma. Smooth muscle cells are connected end to end through dense bodies which are similar to the z disks. These dense bodies have structures made of intermediate filaments and tethering proteins that aid in stably connecting the cells together. Some intermediate filaments also wrap around the muscles and stabilize their structures. (Betts et al., 2013).

Contraction of smooth muscle cells starts upon stimulation which leads to calcium influx inside the cell from calcium channels on the sarcolemma and sarcoplasmic reticulum. The calcium binds to calmodulin which activates an enzyme called myosin light chain kinase which phosphorylates the myosin light chain to activate it (Aguilar and Mitchell, 2010). Since the myosin light chain is near the head, its activation leads to the activation of the head and initiation of contraction.

Heart muscle cells are like skeletal muscle cells with the sarcomere being the basic functional unit in the cell. The T tubules are at the z disks, with one T tubule per sarcomere, unlike skeletal muscles where there are two T tubules per sarcomere occurring at the I and A band junctions. Heart muscle cells are bound by intercalated discs which form tight junctions through desmosomes that hold the muscles together during contraction. They also have gap junctions which work as networks to keep the cytoplasm of different cardiomyocytes connected as one unit (American Heart Association, 2012).

In the heart, muscle cells are majorly organized in the myocardium layer, 99% of which are contractile and 1% work to initiate and conduct the electrical current. As heart muscle cells increase their pumping rate, they grow by adding more proteins, a process

called hypertrophy; it also happens in the skeletal muscle cells. This explains why an athlete's heart can pump more efficiently than nonathlete heart at rest. It is noteworthy to mention that heart muscle cells have similar amino acid sequence to the skeletal muscle cells but not to the smooth muscle cells. (Goodson and Spudich, 1993)

1.2 The Sarcomere and Its Proteins (Myosin, Actin, Tropomyosin, Troponin, MyBPC, Nebulin & Nebulette and Titin)

The sarcomere (Fig. 1.1) is the functional unit for contraction in skeletal and cardiac muscles. It extends between two z disks. The I-band (Isotropic) is the region around the z disk that is made of actin without myosin. The A-band (anisotropic) is composed of actin and myosin. The H zone within the A band, is the region made of myosin only, and the M line centers the H zone and the sarcomere. Sarcomeres start assembling at the z disk (Ehler and Gautel 2008; Sanger et al., 2010) where actin is synthesized, capped and crosslinked with α-actinin- see below- (Gautel and Djinović-Carugo, 2016). Sarcomeres are made of multiple proteins including myosin, actin, MyBPC, titin, nebulin, nebulette and several other proteins, some of which are less studied.

The sarcomeric protein Myosin (Fig. 1.1) is composed of a dimer; each monomer is bound by a regulatory light chain (RLC) and an essential light chain (ELC). When a myosin monomer is mildly digested it produces two structures: heavy meromyosin (HMM) and light meromyosin (LMM) (Margossian and Lowey, 1982). The HMM can be further divided into head region where it binds to actin to initiate contraction, and the S2 region which is a flexible neck that magnifies the head movement during contraction. The LMM, on the other hand, is thought to be the less active portion of the myosin. RLC in myosin has a major role in smooth muscle cells, which upon phosphorylation initiates contraction.

In skeletal and cardiac muscle cells, it is the calcium influx that initiates the contraction, but less frequently, the phosphorylation of RLC has been proposed to increase contraction (Toepfer et al., 2013; Levine et al., 1996; Nag et al., 2017) along with the MyBPC phosphorylation.

Actin is another important sarcomeric protein, its filamentous state (F-actin) is a polymer of the globular actin (G-actin). It is barbed at the z disk and capped with a protein called cap-z (Casella et al., 1986; Casella et al., 1987) which aids in the insertion of the actin in the z disk. At the M line, the pointed end of actin is capped with tropomodulin (Tmod). Both proteins help to stabilize the length of the actin by preventing the addition and removal of actin monomers. Actin is a major protein in contraction; in fact, knockout mice for α-cardiac actin die before or right after their birth (Kumar et al., 1997), however, they may survive longer in knockout α-skeletal actin (Harper et al., 2002). Another two important regulatory proteins for actin are tropomyosin and troponin; tropomyosin is composed of a super-helical structure that interacts with the positively charged groove of actin (von der Ecken et al., 2015) and forms a stable complex that prevents the myosin from reaching to actin to initiate contraction. Knockout of the tropomyosin leads to embryonic lethality (Rethinasamy et al., 1998). Troponin, the other regulatory protein that binds to actin, is composed of 3 proteins: troponin I, C and T. Troponin I binds to actin and inhibits its binding to myosin. Troponin C binds to calcium and undergoes conformational change to open the actin for myosin to initiate contraction (Lehman et al., 2001). Troponin T binds to tropomyosin (Potter et al., 1995). When an activation signal is received, the Ca^{+2} is released from its reservoirs and binds to the troponin complex, specifically to troponin C which becomes activated and transfers the signal to troponin I,

offsetting its inhibition on actin and eventually transferring the signal to Troponin T that is bound to tropomyosin. Tropomyosin is the key protein in regulating the availability of actin to initiate contraction through blocking the active sites on myosin. The activation signal shifts the troponin-tropomyosin complex and opens the active site for myosin to initiate a contraction cycle in the presence of mg-ATP. Magnesium is a vital element in initiating contraction through binding to ATP (Romani et al., 2002).

Another sarcomeric protein that is well studied is the MyBPC. The C-end of this protein is thought to bind to the LMM (Flashman et al., 2007; Miyamoto et al., 1999) and sometimes titin (Freiburg et al., 1996) while the N-end is thought to bind to actin, S1 head and S2 (Kulikovskaya et al., 2003; Rybakova et al., 2011; Shaffer et al., 2009; Squire et al., 2003). The binding of the N-terminal end to the S1 head and the proximal S2 turns the contraction off through inducing a bend in the myosin head on S2 to prevent it from participating in contraction (Trivedi et al., 2018), this structure is called the “off state” as described below. This is especially notable when the Ca^{+2} is low and the MyBPC is unphosphorylated (Kamporaukis et al., 2014; Moss et al., 2015).

An additional sarcomeric protein that plays a role in actin regulation in skeletal muscle cells is called nebulin. It was previously known as the actin ruler as its size correlated to actin size (Kruger et al., 1991; Labeit et al., 1991), and its motifs correlated with actin binding sites (Pelin, K. & Wallgren-Pettersson, C., 2008). However, further studies showed that actin may surpass the length of nebulin especially at the N-terminal end, despite interacting with it at the C-terminal end in the Z-disk to regulate both the Z-disk size and the actin length there (Tonino et al., 2010; Witt et al., 2006; Millovei et al., 1998). It is believed that Tmod protein is responsible for regulating the size of actin at the

N-terminal (Gokhin and Fowler; 2013). Nonetheless, nebulin was given the role of actin stabilizer. 50% of nemalin myopathy patients have nebulin mutations that result in muscular degeneration. On the other hand, nebulette, the cardiac relative of nebulin, is responsible for actin stabilization in the heart (Moncman & Wang, 2002). Mutations in the nebulette in humans causes dilated cardiomyopathy (DCM), irregular contraction, shorter actin and cardiac failure (Purevjav et al., 2010; Henderson et al., 2017; Yuen et al. 2020).

Titin, the last in the sarcomeric proteins described here, is the largest polypeptide in the body with approximately 38,000 amino acid residues (Bang et al., 2001). It extends from the z disk to the M line. Its N-end is bound to the z disk and is composed of several domains, including the flexible PEVK domain (Proline, Glutamate, Valine and Lysine) with different multiples of PEVK along the titin sequence. This sequence works as a spring that induces passive force (Gautel and Goulding, 1996; Labeit and Kolmerer 1995; Linke et al., 1996) which resists the pulling from the extended surrounding sarcomeres. In the heart, the PEVK is even shorter inducing further passive tension (Freiburg et al., 2000). At the C-end, where titin binds to the M line, it is thought to bind to the MyBPC. Mutations in titin have been linked to dilated cardiomyopathy (Herman et al., 2012).

1.3 Stability of the S2 and Heart Disease

It is hypothesized that myosin S2 is a flexible region that allows myosin heads to reach actin and initiate contraction (Huxley et al., 1971; Root, 2002; Li et al., 2003). S2 is more flexible than other coiled coils, reaching up to 2.5 its original length at almost 20-25 pN when stretched, then reversibly transitioning into its original state in less than a second (Schwaiger et al., 2002; Root et al., 2006). In protein digestion assays, the S2 is highly digestible at its hinges suggesting more exposed residues due to weak compacting

(Burke et al., 1973). Even previous attempts to solve X-ray crystal structure of the S2 region revealed that it is flexible and poorly ordered at the hinges (Li et al., 2003). The importance of S2 in contraction was demonstrated through a polyclonal antibody that was raised against the S2 dimer causing the actin to cease movement in the in vitro motility assay (Margossian et al., 1991), other antibodies that were raised against the S2 monomer such as the MF30 caused an increase in contraction (Bader et al., 1982).

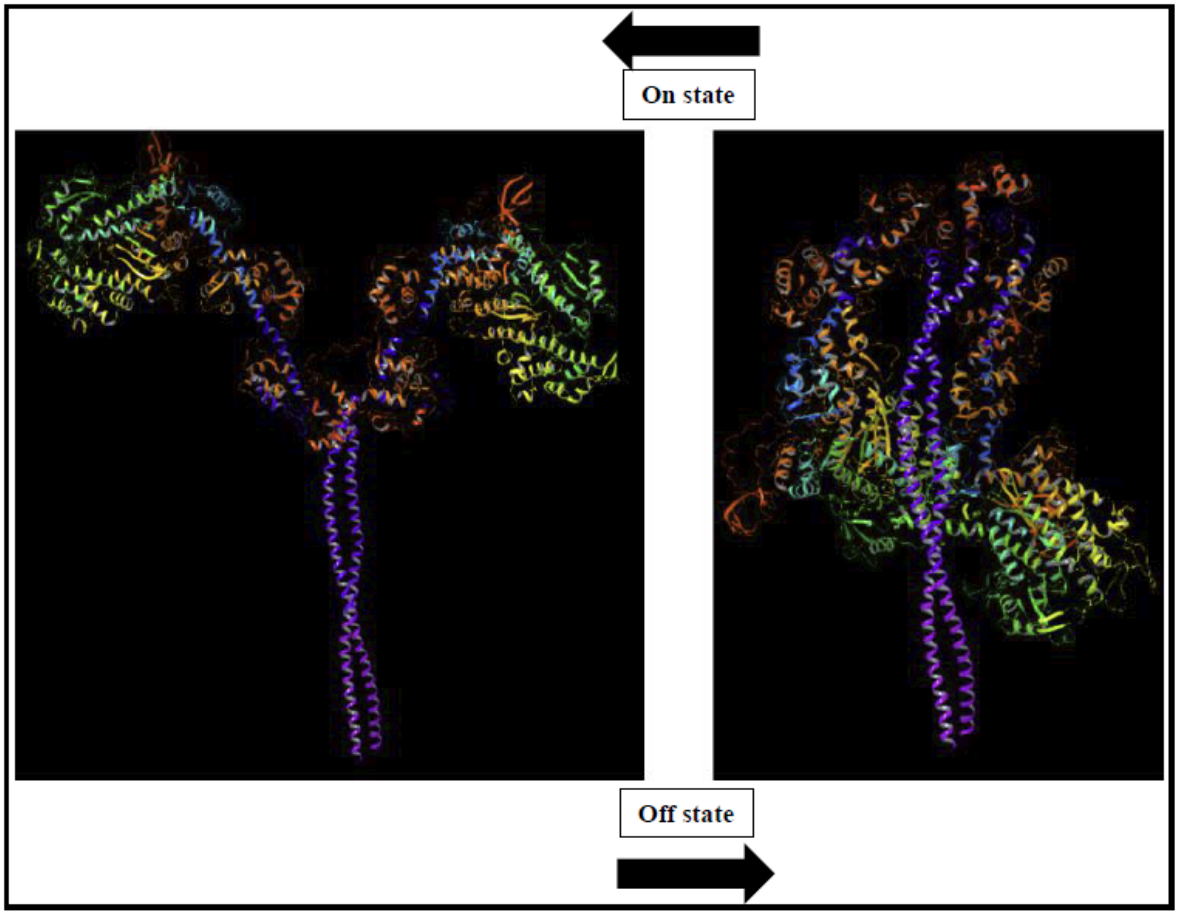

Figure 1.2: On and off states of myosin heads. The heads are in the open conformation to the left (on state), while they are in the closed conformation to the right (off state). (Original structure (5TBY) was imported from PDB).

Some familial hypertrophic cardiomyopathy (FHCM) mutations can increase S2 flexibility such as the case in the E930del, leading to hypercontractility, enlarged heart muscle cells, myofilament disarray, fibrosis, arrythmia and sudden death (American Heart

Association, 2020). The E930del may become fatal occasionally, it may disrupt the heptad repeat of the alpha helix dimer. It is also thought to break some salt bridges that stabilize the myosin dimer, which further contributes to weakening of the dimer bond. A third theory suggests that these mutations disrupt the interaction between the myosin heads and the nick region, more specifically mutations in arginines in the mesa region of the head (Spudich 2015) and mutations in the negatively charged amino acids in the S2 region (Hamburger et al., 2016) will cause FHCM. According to the myosin mesa theory, in resting WT myosin, the heads bend back on the S2 region with the assist of the MyBPC in what is called the “off state” rendering them unavailable to initiate contraction as shown in (Fig. 1.2), however, in the presence of a mutation that disrupts this interaction, the number of available myosin heads that engage in contraction “on state” will increase leading to FHCM (Adhikari et al., 2016; Kawana et al 2017; Nag et al., 2015; Spudich et al., 2016).

Any of the above theories, or rather a combination of them all is not yet determined as the major cause of FHCM in S2 mutations. The FHCM, however, in many occasions, is not due to mutations in the S2 region, there are other mutation hotspots in the myosin head, MyBPC and titin (Walsh et al., 2010; Colegrave et al., 2014; Alcalai et al., 2008; and Seidman 2000; Seidman 2000, Blair et al., 2002).

Hypercontractility and other associated symptoms of FHCM eventually lead to an increase in the thickness and stiffness of the heart wall which renders the heart unable to hold and pump enough blood. By definition, these are the symptoms of heart failure, which in the bigger context is described as reduction in the heart ejection fraction (EF). In another contrasting case of heart failure, heart walls thin and the inner chambers enlarge

leading to reduced pumping ability of the heart (DCM). Both types of heart failure are caused by diabetes, high blood pressure and alcohol, however the FHCM heart failure is mostly inherited.

Since FHCM is usually associated with hypercontractility, a drug with the potential to stabilize the S2 and reduce contractions may partially balance this complication. This molecule may not be as effective for mutations in the head region. In contrast, a drug should aim to increase heart contractions by destabilizing the S2 region to counteract weak pumping in DCM hearts and other heart dysfunctions that reduce contractions.

1.4 Stabilizer and Destabilizer

After closely studying the instability of the S2 region in some FHCM mutations, particularly the E930del mutation, a long stretch of negatively charged amino acids that repulse each other in the dimer were found. This prompted the thought about a positively charged molecule that would wrap around the negative charges to stabilize them, thus came the stabilizer concept (Singh, 2017; Aboonasrshiraz 2020).

On the other hand, to reverse some of the heart failure symptoms resulting from DCM, a molecule was designed to outcompete the bonds between the myosin strands to prevent their dimerization, causing instability in the S2 region and a release of the off state (Singh, 2017; Aboonasrshiraz 2020); the molecule was named the destabilizer. It was specific to the S2 region because part of the S2 was included in the design. The destabilizer was aimed to disrupt the S2 region leading to freedom of movement of the myosin heads to reach actin and initiate contraction. (From here on, whenever the stabilizer and destabilizer are mentioned together, they will be called “anti-myosin S2 peptides”).

The use of peptides as potential drugs has been widely applied in literature, for example, peptide drugs have been designed against the HR1 region in the spike protein of SARS-CoV-2 to prevent it from penetrating the host cells (Xia et al; 2020). My research also used the spike protein sequence to build destabilizers against the HR2 sequence of the SARS-CoV-2 (Qadan et al., 2021). Another example is the delivery of a p53 activator peptide (Joshi et al., 2013) which blocks metastasis of breast cancer cells. Many other peptide drug models can be found in the literature, in fact, there were 400 peptide drugs that were under clinical trials by 2019, while 60 more were approved (Lee et al., 2019).

1.5 Cell Penetrating Peptides and Heart Homing Adducts

Some peptide adducts were developed to assist penetrating cellular membranes, but they are not specific, these are called cell penetrating peptides (CPP). Tat protein domain of the HIV (Frankel et al., 1988; Green et al., 1988) and the poly acidic amino acids such poly Arginine (Wender et al., 2000) and poly Lysine (Mai et al., 2002) are examples of such non-specific CPPs. Other adducts are more specific where the phage display method is used for screening. In this method, the phages are engineered to display query proteins on their surfaces, then they are allowed to interact with the desired tissue (cancerous, heart, etc..) to determine their ability to internalize in the tissue. The viruses are then collected and tested again to determine false positives. The screening process is repeated 4-5 times to identify phages with true abilities to bind and internalize inside the tissue (Zahid et al., 2011).

Since the anti-myosin S2 peptides are designed against the heart myosin, they should be able to pass through heart cells. The stabilizer may be able to penetrate cells in general, but it is not target-specific. The destabilizer, however, may have neither ability.

Therefore, a search was conducted to find a molecule that would aid in penetrating heart cells without imposing functional challenges to the peptides. Several adducts that bind covalently to the anti-myosin S2 peptides were found. Recently, however, a paper introduced tannic acid (TA) as being target specific adduct that can bind and deliver molecules to the heart including GFP, viruses and other peptides (Shin et al., 2018). TA is thought to bind to the extracellular matrix proteins of the heart which might be aided by the 25 hydroxyl groups that can form hydrogen bonds with the cargo and the target. Therefore, the work was redirected towards the use of TA due to its simple binding reaction with proteins, its availability, reduced toxicity to the heart and most importantly its confirmed results. TA is structurally made of glucose and galloyl moieties. Synthetic TA is made of 10 galloyl moieties, however, the naturally occurring ones can have varying number of attached moieties. In electrospray mass spectroscopy, TA has high tendency to break apart and show a spectrum containing all possible bonding patterns ranging from glucose alone to glucose bound to multiple galloyl moieties; thus, it is one of the harder molecules to determine its binding pattern to other proteins and peptides.

1.6 Hypothesis and Testing

My work involved testing the instability of the S2 region which aids in propagating contractions. Based on its pivotal role, two models were built to modulate S2 dynamics: the stabilizer and destabilizer. The destabilizer is a peptide that disrupts the S2 region to induce more contractions, while the stabilizer stabilizes the S2 region to reduce contractions. The efficiency of the stabilizer and destabilizer was determined using computational chemistry and wet lab tests on myofibrils (Singh, 2017). After enough evidence had compiled, they were prepared for cell culture and animal model tests. It was

important to maintain their functionality during the modification process that aided in their internalization inside the cardiomyocytes. Multiple adducts were tested and eventually TA was picked, while still reserving a stock of other heart homing peptides that covalently attach to the anti-myosin S2 peptides**.** These were the second option in case TA did not pass the animal model tests.

To organize the work above, it was put into a testable hypothesis as follows: contraction output can be tuned by modulating the flexible S2 region through anti-myosin S2 peptides which can append to heart homing adducts without noticeable effect on their functionality. This hypothesis was organized into 3 aims: in the first aim, S2 instability was studied, then anti-myosin S2 peptide models were built and their efficiency in modulating S2 instability was determined. This aim was the longest, thus, it was divided into two sub-aims. In the first sub-aim, the instability of the S2 region was tested and compared to other myosin regions. To commence this task, simulated force spectroscopy (SFS) was performed on different parts of myosin: the myosin head, S1-S2 junction, S2 and LMM. The process involved pulling the myosin from one end one Angstrom at a time until it was fully separated. The parts of myosin that required more force to pull were considered stable, while the parts that required less force were considered unstable. In the second sub-aim, different lengths of stabilizer and their efficiency in binding to FHCM models were investigated, while different models of the destabilizer were proposed. The competent length of the stabilizer with the potential to wrap around the myosin was determined using SFS simulation. While Dynamic simulation was used to confirm the stabilizer's ability to remain attached to E930del at conditions similar to the human body temperature at 310 Kelvin. Helical content of the stabilizer-E930del complex was

determined using Ramachandran plot to confirm the stabilizer's ability in retrieving myosin S2 helicity.

In building the destabilizer model, SFS was used to determine the cornerstone amino acids in holding the myosin S2 together. The destabilizer should overcome these bonds and bind S2 to prevent myosin dimerization. The bond strength between the destabilizer and the myosin was determined using the "interaction energy". Here, molecules were energy-minimized, and the value was recorded, then they were separated, and the value was recorded again. The difference in these values was the interaction energy, which can also be thought of as the energy released upon reacting two or more molecules together. The more negative the value, the stronger the bond. The interaction energy of the destabilizer-myosin was compared to WT myosin dimer bond.

In the second aim, different adducts that aid in homing the anti-myosin S2 peptides to the heart were computationally tested using the interaction energy assay to determine their influence on the anti-myosin S2 peptides functions. TA showed the highest potential among the adducts, thus it was tested for its ability to bind to anti-myosin S2 peptides using mass spectroscopy. The results were compared to the spectra of anti-myosin S2 peptides alone and TA alone to determine bond formation between the TA and the anti-myosin S2 peptides. Then the TA-anti-myosin S2 peptide complex was purified from the unbound TA to reduce potential toxicity ensuing from TA. However, since the purification step turned non-effective, unbound TA was lowered through reducing the starting TA concentration in the TA : anti-myosin S2 peptide reaction.

In the third and last aim, I needed to determine whether TA in the TA-anti-myosin S2 peptide complex affected the anti-myosin S2 peptide in vitro or not. To investigate this,

the position of the TA-anti-myosin S2 peptide complex in the sarcomere was determined through expansion microscopy and compared to anti-myosin S2 peptide alone to determine whether the TA interfered with the complex position or not. Then the TA-anti-myosin S2 peptide function was tested through contractility assay and compared to anti-myosin S2 peptide alone. In this assay the amount of contraction was measured through sarcomeric shortening upon the addition of ATP.

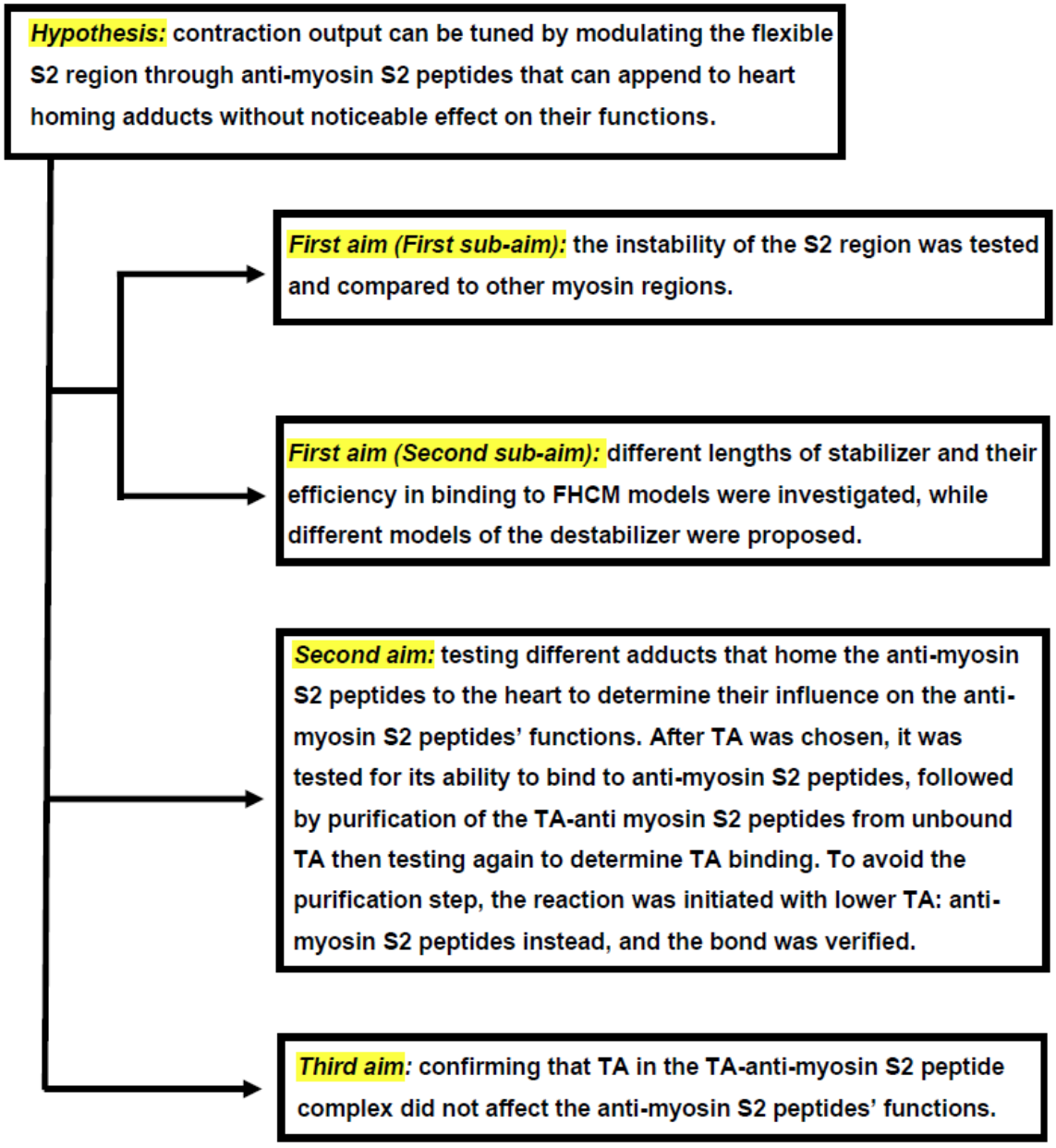

CHAPTER 2

MATERIALS AND METHODS

2.1 Materials

2.1.1 Myofibrils

Myofibrils were extracted from a rabbit back and psoas muscles. Almost 20 grams were suspended in 200 ml of buffer (20 mM potassium chloride, 10 mM bis-tris and 4 mM EDTA at pH 6.8) at 4 ^{o}C. The sample was then homogenized using a blender at high speed for 5 seconds. The homogenate was then washed three times; 600 mls each time using the same buffer. Each wash involved centrifugation and removal of the supernatant. In the last step of washing the pellet was suspended in the same buffer containing 50% glycerol then it was reserved in the -20 ^{o}C freezer (Root, D.D. and Reisler, E. 1992; Godfrey J.E. and Harrington W. F. 1970)

2.1.2 Stabilizer

Computational chemistry was used to design the stabilizer molecule which contained high proportionality of positive amino acids that can bind negative residues on myosin. To induce the stabilizer to wrap around the myosin, a bent was introduced into its structure by substituting some of its amino acids. The stabilizer was chemically synthesized by Bio-synthesis Inc., Lewisville, Texas, United States.

2.1.3 Destabilizer

The destabilizer (DE) was also designed in our lab to compete with myosin dimer formation. Computational chemistry and data from antibodies that destabilize the S2 region were used to build the sequence. The design incorporated myosin S2 sequence with some modifications to increase its competition with the myosin dimer. The

destabilizer was chemically synthesized by Bio-synthesis Inc., Lewisville, Texas, United States.

2.2 Methods

2.2.1 Computational Chemistry

Myosin S2 (2FXO) was imported from protein data bank, then it was cropped and fixed using Maestro 9.0 for use in computational chemistry. Two simulations were carried out: molecular mechanics and molecular dynamics. Molecular mechanics included two measurements: simulated force spectroscopy (SFS) and interaction energy. Molecular dynamics simulation, on the other hand, involved observing peptides' interactions with other peptides or alone in solution over time at a certain temperature. The first step in all simulations (mechanics or dynamics) was to energy-minimize the peptides through several cycles of minimizations and conformational searches using OPLS_2005 force field. Minimization was run to convergence at 0.05, or 10000 iterations, while conformational search was run to convergence at 1.00, or 1000 iterations using mixed torsional/large scale low mode sampling method.

In molecular mechanics' SFS simulation, two atoms from corresponding amino acids on each strand were picked, and the distance separating them was measured. The distance was then increased 1 Å one at a time until the two molecules were completely separated. The actual separation was less than 1Å due to the attraction between the strands. This behavior is similar to spring behavior where it would be at rest if the two strands had separated the whole 1 Å, however, the spring would compress an amount of X due to the attraction forces between the atoms. The potential energy in the "spring" is

the amount of force holding the molecules together. It can then be calculated according to Hook's law as follows:

$$F = KX$$

where F is the spring potential force. X is the difference between the intended and the actual separation distance. K is the spring constant which is 1661.13 pN/ Å and was determined experimentally (Root et al., 2006). The amount of force required to separate the whole molecule was integrated to give the total force.

SFS was performed on different WT myosin locations to determine the stability of the S2 compared to other regions of myosin. Four positions were picked for pulling: N-terminus, S1-S2 hinge, post-hinge (S2 position) and LMM position. SFS was also performed on WT myosin to determine the major amino acids that hold it together, which later was used to build the destabilizer model. SFS was also carried out on E930del with different lengths of polylysine (12, 17, 21 and the modified polylysine) to determine the one with the best stabilizing effect.

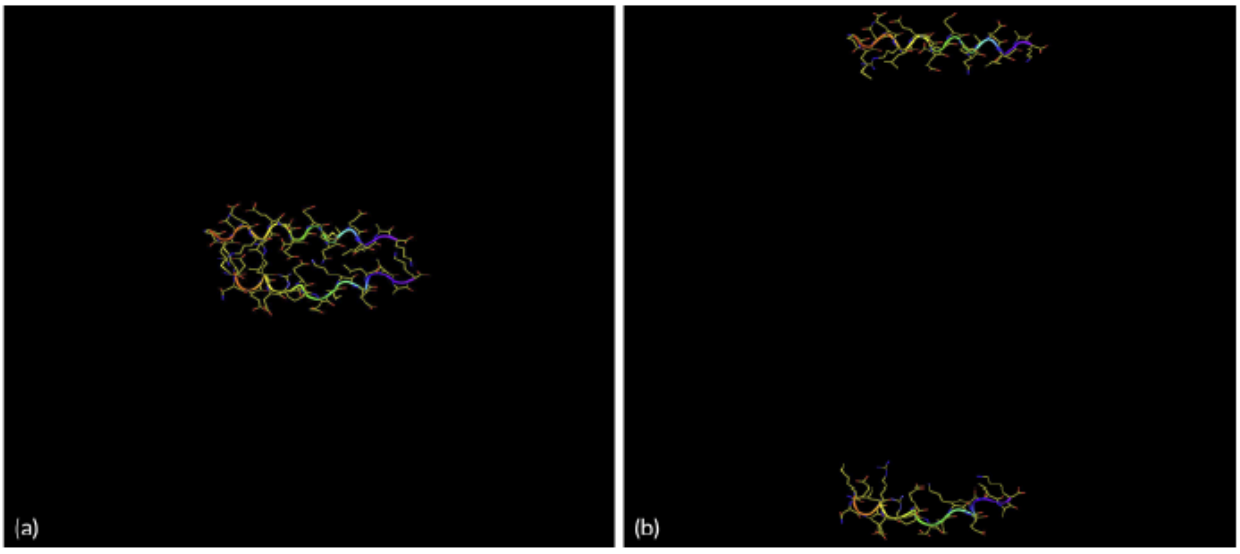

Figure 2.1: Illustration of interaction energy measurement. (a) The molecule was minimized to its minimum energy. (b) The molecule was separated then minimized. The difference between the energy of the separated and the joined molecules is the interaction energy.

Molecular mechanics' interaction energy (Fig. 2.1) was measured through reacting 2 molecules together to their minimum energy then recording their energy value. The molecules were then physically separated from each other and their energy value was recorded again after running minimization search. The difference between the two values was the interaction energy, which was used to determine the force that held the destabilizer with myosin S2, and it was also used to choose among the different heart homing adducts that attach to anti-myosin S2 peptides.

In molecular dynamics simulation, the samples were run for 16 ns at 310 K using stochastic dynamics. The structures were run to convergence at 0.05 or 10000 iterations. 1000 structures were sampled from each simulation. Dynamic simulation was used to determine the interaction of the E930del with the solution over time and compare it with the WT and E930del with stabilizer.

Following molecular dynamics simulation, the helical content of the structures was determined using Ramachandran plot. Out of the 1000 structures recovered, the helical content was studied for 80 structures sampled over the whole simulation period. The structures were then averaged to 8 and plotted. Amino acid that fell in the red zone around the angles φ= -57° and ψ= -47° were considered part of α helical fold.

2.2.2 Crystallizing Myosin S2 with the Stabilizer

It was attempted to crystallize the stabilizer with myosin S2. The concentration of the peptide was 1 mg/ml, while the rest of the conditions in the 24 plate were as follows:

	PEG 3350 15% Tris	**PEG 3350 15% Tris**	**PEG 3350 20% Tris**	**PEG 3350 20% Tris**	**PEG 3350 25% Tris**	**PEG 3350 25% Tris**
pH 6.5	0.2 M Na acetate	0.2 M Citrate	0.2 M Na acetate	0.2 M Citrate	0.2 M Na acetate	0.2 M Citrate

	PEG 3350 15% Tris	PEG 3350 15% Tris	PEG 3350 20% Tris	PEG 3350 20% Tris	PEG 3350 25% Tris	PEG 3350 25% Tris
pH 7.5	0.2 M Na acetate	0.2 M NaCl	0.2 M Na acetate	0.2 M NaCl	0.2 M Na acetate	0.2 M NaCl
pH 8	0.2 M Na acetate	2 M Citrate	0.2 M Na acetate	0.2 M Citrate	0.2 M Na acetate	0.2 M Citrate
pH 8.5	0.2 M Na acetate	0.2 M NaCl	0.2 M Na acetate	0.2 M NaCl	0.2 M Na acetate	0.2 M NaCl

Unfortunately, no crystals were found under these conditions, although they were close to the myosin S2 crystallization conditions (Blankenfeldt et al., 2006)

2.2.3 Mass Spectroscopy and Tannic Acid Conjugation to Peptides

Mass spectroscopy is used to determine different components of mixtures whether they are in the solid, liquid or gaseous states. It works by measuring the mass to charge ratio. There are four major components for the mass spectroscopy machine: inlet, ionizer, analyzer and detector. Direct injection was used as the inlet route for the samples, while the electrospray equipment ionized them. Ionization in electrospray involves thin pins that create small charged droplets which dehydrate as they fly to the opposite pole causing the charge density to increase. Eventually the overwhelmingly charged molecule explodes producing smaller charged ions, which can be segregated based on their mass to charge ratio as they fly to the detector. QuanTOF analyzer was used to analyze the TA-anti-myosin S2 peptide samples, while other mass spectroscopy techniques such as MALDI-TOF can be used to produce less complex spectra.

In this experiment, mass spectroscopy was used to determine whether TA was able to bind to anti-myosin S2 peptides or not. If the compounds being tested were unknown, then the sample could be run, and the results could be compared to a database

of runs to determine if there was a peptide or protein with results similar or identical to the query run. In the TA-anti-myosin S2 peptides case the molecules were known, however, the peaks they produced were unknown because they were not in the database. Therefore, a different approach was followed to determine bond formation between TA and anti-myosin S2 peptides. Here, TA was run by itself and the results were recorded, then the anti- myosin S2 peptides were run by themselves and the results were recorded, then both molecules were run together, and the new peaks were explored. These peaks would be expected to represent the bonds between the anti-myosin S2 peptides and TA if they show up consistently and correspond to the m/z ratio of the TA-anti-myosin S2 peptides complex. To apply this in practice, TA was mixed with anti-myosin S2 peptides at 10:1 ratio. The stabilizer-TA and destabilizer-TA were prepared by shaking the samples vigorously for 3 nights in PBS (0.137 M NaCl, 0.0027 M KCl, 0.01 M Na_2HPO_4, 0.0018 M KH_2PO_4 at pH 7.1) then they were analyzed by mass spectroscopy. Before injection into the machine (SYNAPT G2-Si High-Definition Mass Spectroscopy from Waters), samples were first pipetted with zip tips C18 matrix for 3 times, then 20 µls of sample were added to 479 µls of 1 : 1 acetonitrile to water (volume) solution to which formic acid was added to 0.2% final concentration. The machine was first linked to liquid chromatography, and a reverse phase column C18 was used for separating the samples, however, because the samples clogged the column, they were directly injected into the column instead. The above procedure was also followed when TA alone, anti-myosin S2 alone and samples from purifying the extra unbound TA from the TA-anti myosin S2 peptides were tested.

2.2.4 Purification of TA-Anti-Myosin S2 Peptides from Extra Unbound TA

When dealing with myocytes, a purified sample of TA-anti-myosin S2 peptides

should be prepared to avoid any toxic side effects from TA. Purification was carried out in two steps: ion exchange chromatography (IEC) and gel filtration. In IEC, NaCl was gradually incremented to 1 M NaCl over 20 mls to avoid sharp increase of salt concentration. Then gel filtration was used to desalt the sample at a flowrate of 1ml/min. Later, however, IEC was excluded from the procedure to avoid the loss of the expensive anti-myosin S2 peptides in this step, which did not noticeably improve the purity anyhow. Therefore, a G-10 gel filtration column was packed to filtrate the samples manually (3 inches long and 3 quarters of an inch in diameter). The samples were dispensed on the top of the column and were washed with PBS buffer as the mobile phase. The elution was then collected in 0.5 ml fractions.

2.2.5 Bicinchoninic Acid Assay and Fluorescamine Assay for Measuring Concentrations

The phenylalanine amino acid in the stabilizer has a distinguishable absorption peak at 259 nm. The destabilizer on the other hand, can only be measured using the absorption of peptide bonds, which sometimes can be difficult to perform. Otherwise, the peptide can be accurately weighted and added to an accurate amount of buffer so the concentration can be precisely determined. When TA was mixed with either the stabilizer or destabilizer in this experiment, its absorption peak overrode the absorption of phenyalanine and peptide bonds. Therefore, to approximately determine the concentration of the peptide sample, an assay called bicinchoninic acid assay (Smith et al., 1985) was used. In this method 3 solutions were prepared:

- -Solution A is 0.8% NaOH, 1.9% sodium bicarbonate, 0.32% sodium tartrate, 4% sodium carbonate
- -Solution B is 4% bicinchoninic acid
- -Solution C is 4% cupric sulfate

Solution A provides an alkaline environment (pH 11) that allows proteins to reduce Cu^{+2} into Cu^{+1}. The Cu^{+1} then binds to two bicinchoninic acid molecules present in solution B turning them into purple, which provides a colorimetric method to quantify the proteins. Because the BCA technique was shown to be affected by TA concentration, another technique called the fluorescamine assay (Win et al., 2012) was used, which detects minute amounts of proteins by reacting with primary amine groups. The assay solution was prepared by mixing 3 mg of fluorescamine in 1ml DMSO, then the fluorescamine-DMSO solution was mixed with the sample at a proportion of 1 volume fluorescamine : 3 volumes of sample and measured with the spectrofluorometer device.

2.2.6 Contractility Assay

This technique was used to measure the amount of contraction the myofibrils underwent upon the addition of ATP in the presence of anti-myosin S2 peptides or other muscle modulators. In this procedure the myofibrils were washed using the contractility assay buffer (0.1 M potassium chloride, 0.5 mM calcium chloride, 3 mM magnesium chloride and 50 mM immidazole) 3 times to remove any residual glycerol. It is recommended to shake the myofibrils for a minute between washes or pipette up and down without over shaking or running high-speed centrifugations as contractions might be disturbed. The samples were prepared by vigorously mixing TA with anti-myosin S2 peptides at 10 : 1 concentration for 3 nights in PBS. Then myosin was incubated with TA-anti-myosin S2 peptides overnight at low speed rocking. The peptides were then investigated under the microscope by spreading a mixture of 99 µl of the buffer and the myofibrils on a microscopic coverslip. An image was obtained for the relaxed myofibrils through the 40X (NA=1.2) water immersion c-apochromatic objective lens by a camera

mounted on an inverted microscope. Next, ATP was added to a final concentration of 1 mM to allow the contraction to occur imminently, then an image was taken again. The images before and after contraction were analyzed using a program called ImageJ developed by the NIH to determine the amount of sarcomeric shortening as an indicator of contraction according to the following equation:

The amount of contraction = (Difference of sarcomere length before and after contraction / Sarcomeric length before contraction) X 100%

It is noteworthy to mention that upon adding an ATP drop, some of the myofibrils stir and move up or down the field of focus, which may deceive the observer as being contraction, but it is not a true one. Another noteworthy observation was that not all myofibrils showed detectable contractions, in fact many of them did not contract, possibly because they might be stuck to the glass underneath them, or they might be old or non-functional. Lastly, it was remarkable to notice that contraction could not be initiated without high Mg^{+2} concentration as ATP might bind to Ca^{+2} in the event of short supply of Mg^{+2} ions, sequestering Ca^{+2} from binding to myosin to initiate contraction.

2.2.7 Purification of Stabilizer-TRITC from Unbound TRITC and Purification of Destabilizer-FITC from Unbound FITC

To prepare the anti-myosin S2 peptides for expansion microscopy, TRITC and FITC were used as fluorescent dyes, where both were processed in the same manner. They were first dissolved in DMF, then they were reacted at equimolar concentrations with anti-myosin S2 at 1:1 ratio in PBS buffer at pH 7.4 to achieve equal binding. After shaking for 1 hour at room temperature, a reverse phase column pepRPC was used to separate the unbound dyes from the labeled anti-myosin S2 peptides. Solution A was 0.05% TFA in water and solution B was 0.05% TFA in acetonitrile. The flowrate was .1

ml/min with gradual increase in solution B from 0% to 100%. TFA at low concentrations is considered an ion pairing agent which is an agent that binds to counter ions to neutralize them. In this case, the TFA neutralized the stabilizer and destabilizer making them more hydrophobic when bound to the dye as a complex than the dye by itself. Thus, unbound dyes would come out first with water mixed with little acetonitrile, followed by the anti-myosin S2 peptides-dye complex which would elute later with high concentrations of acetonitrile. Then a second reverse phase step with a 5 mm x 20 cm divinylbenzene column was applied to remove the acetonitrile since it could affect the samples. Here, solution A was water, and solution B was methanol. As water was pumped through the column it pushed the acetonitrile out while the peptide remained attached. When methanol was pumped however, it eluted the TRITC-anti-myosin S2 peptides complex. Then it was evaporated to leave the water behind as a solvent for the peptides. After the peptides eluted from the chromatography column, the concentrations of the peptides bound with FITC or TRITC were calculated as follows:

*Protein concentration= **(**(A of the peptide-dye complex at 280) - **(**(A of the peptide-dye complex at 495 for FITC or 555 TRITC) X (A of the dye alone at 280)**)**)/E*

where A is the absorbance, while E is the extinction coefficient for the dye.

2.2.8 Expansion Microscopy

Expansion microscopy is a technique that was developed recently (Chen et al., 2015) as a cheaper alternative for the more expensive and laborious super resolution microscopy. In this technique the gel containing the sample expands upon absorbing water causing it to distance the fluorescent molecules apart, thus improving resolution. The procedure was carried out as following: the fluorescent anti-myosin S2 peptides were mixed with TA at a concentration of 1 peptide : 10 TA (molarity) for 3 days at room

temperature. Then the fluorescent TA-anti-myosin S2 peptide sample was mixed at 0.8 µM with the myofibrils (around 100 µls) in PBS and allowed to incubate in the fridge for 3 days. It is advised to pick small myofibrils and shred them into smaller pieces. On the preparation day, the myofibrils were centrifuged, and the PBS was removed. Then 300-500 µl of diluted glutaraldehyde to 0.1% (some stock glutaraldehyde have 25% concentration) in PBS was added to the myofibrils for 1 hour at room temperature. The glutaraldehyde cross links the fluorescent peptides to the hydrogel and cross links the fluorescent peptides to the myofibrils. Glutaraldehyde was then washed with PBS 3 times, followed by incubating the myofibrils with almost 200 µl of monomer solution for 1 hour at 4^{o}C. The monomer solution was prepared as follows:

Table 2.1: Components of monomer solution for expansion microscopy.

Component	Stock concentration*	Amount (mL)	Final concentration*
Sodium acrylate	38	2.25	8.6
Acrylamide	50	0.5	2.5
N,N′-Methylenebisacrylamide	2	0.75	0.15
Sodium chloride	29.2	4	11.7
PBS	10x	1	1x
Water		0.9	
Total		9.4**	

*All concentrations in g/100 mL except PBS. (The table is obtained from Dr. Andrea Bernardino-Schaefer. The original concentrations were obtained from Zhao et al., 2017)

It is suggested to prepare 10 ml of each monomer solution component (stock concentration). It is also suggested to prepare 400 µl of the monomer solution for each experiment, 200 µl for the priming and 200 µl for the gelation step. The monomer solution is supposed to prime the myofibrils for the gelation step, which followed the monomer

solution incubation. After incubation, the myofibril-monomer tube was centrifuged, and the myofibrils were spread on a slide chamber where the polymer solution was poured over them. The chamber was then covered with a coverslip to allow the gel to form. The polymer solution is similar to the monomer solution with few additions: 4-hydroxy-TEMPO was added to a final concentration of 0.01%, TEMED was added to a final concentration of 0.2% and APS was added to a final concentration of 0.2%. One can prepare the solutions in the following stock concentrations: 10% APS (can be saved for 1 month in the -20 freezer), TEMPO 0.5% (can also be saved in the -20 ^{o}C freezer) and 10% TEMED (which can be saved in the fridge). The polymer solution was prepared by the addition of 4 µls from each of the three solutions above to 188 µl of the monomer solution to make a total of 200 µl polymer solution. The chemical component in the solution that is responsible for absorbing water and expanding the gel is sodium polyacrylate, while TEMPO slows down gel formation so that it can intercalate between the myofibrils. The gel may take 2 hours or a little more to form. If it does not form by then, 2µl of APS and similar amount of TEMED can be added to form a gel. The longer it takes the gel to form, the more the expansion -up to a certain level where no more expansion can be achieved. If the gel forms quickly and no expansion is detected, it is advised in the following attempts to incubate the myofibrils for 2 hours in the monomer solution, exchange it with a fresh monomer solution then incubate again for another 2 hours before adding the TEMPO, APS and TEMED. In this experiment, after the gel formed, it was removed to a weigh boat, and 3 mls of digestion buffer were added to it with 5 µl (around 40 units) of the Pro-K solution. They were incubated overnight at 40 ^{o}C. The digestion buffer components are: 50 mM tris pH 8.0, 1 mM EDTA, 4 M urea, 2 mM $CaCl_2$, 0.05% triton X-100, 0.8 M

guanidine HCl. The digestion buffer can be left at room temperature for about 1-4 months. On the following day, the gel was removed to a big petri dish and soaked in distilled water then washed for 3 times with 20-30 minutes interval, totaling 1-1:30 hour. The gel became expanded ten times or more its original size. 3 µl of polylysine was used to coat each slide before mounting the gel to prevent its drifting while moving the microscope stand. The images were taken by a spinning disc confocal microscope at 40X (NA=1.2) water immersion c-apochromat objective lens with a tube lens of 1.6X.

CHAPTER 3

COMPUTER SIMULATION RESULTS

3.1 S2 Instability

S2 stability was measured using SFS and was compared to LMM. The atomic models were pulled in opposite directions from 4 different positions [Figs. 3.1 & 3.2(a)]: The first position was the N-terminus for the pre-hinge position [Fig. 3.1(a)]. The second was E875 to simulate where MF30 antibody binds on the S1-S2 hinge [Fig. 3.1(b)]. The third was E927 to simulate where the site-specific polyclonal antibody binds on S2 [Fig. 3.1(c)], which is considered a post-hinge position. The last was K1392 in the LMM region [Fig. 3.1(d)]. The same amino acids were picked on both helices to initiate the pulling, then the results were fit to the logarithmic equation:

$$F = a \ln (x + b) + c$$

where a = v *kB* T (v is a proportionality constant (in units of distance−1) and *kB* is Boltzmann's constant. The term (x + b) replaces x in the derived equation because b represents the length of the linker elements such as the antibodies. The term c is -∫ dH/∫ dx which represents the change in enthalpy over distance, which was linear in the results indicating that it could be approximated with a constant value. The change in enthalpy was based on the no. of hydrogen bonds that were broken as myosin was pulled [Fig. 3.1(e, f, g & h)].

The fit data in Fig. 3.2(b) shows that the LMM required high force to separate, which is consistent with the previous data from the gravitational force spectrum. The S2 on the other hand required less force than LMM as shown in the same figure, indicating that it was more flexible and easier to break.

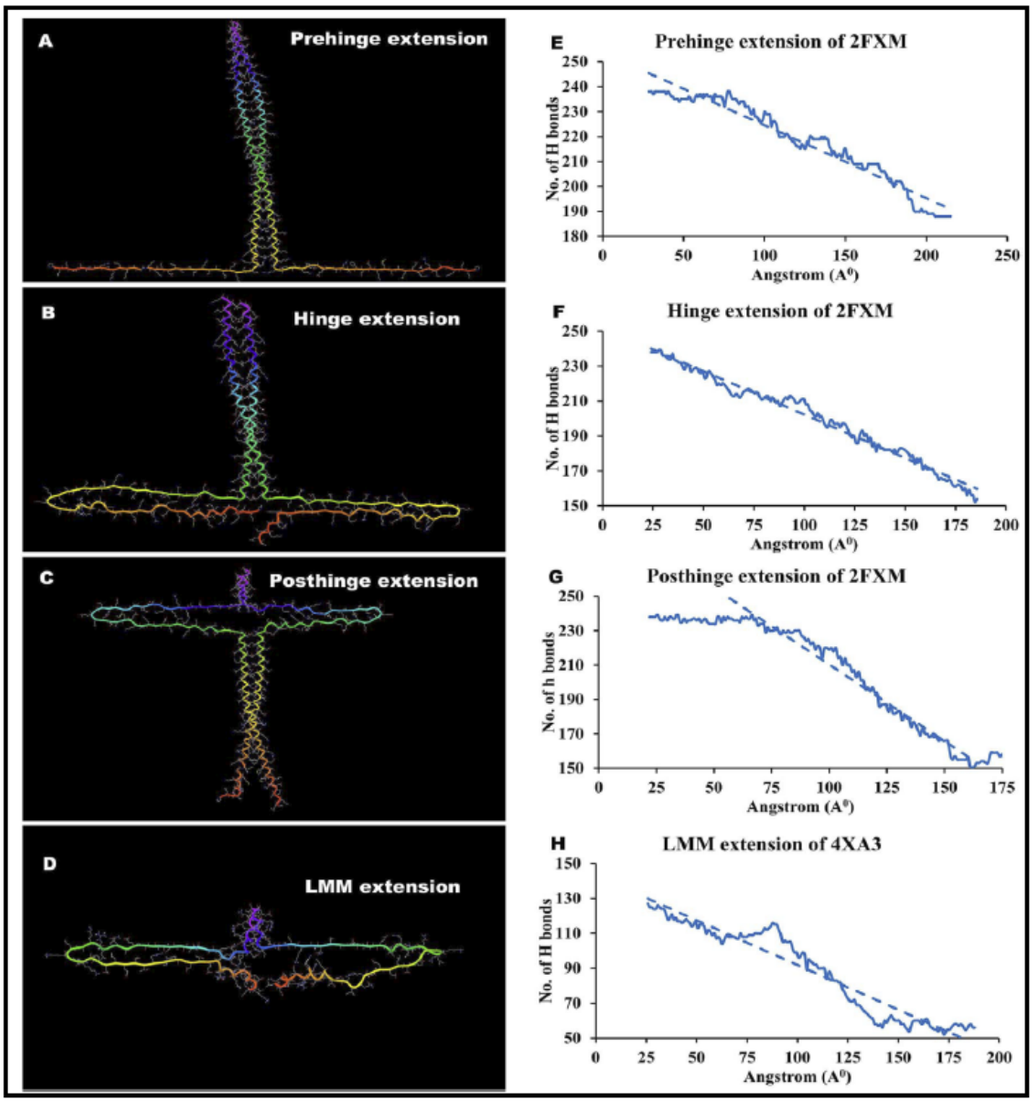

Figure 3.1: The left panel is a depiction for the pulling sites and the right panel is the number of H-bonds with distance. (A and E) correlate to the pre-hinge pulling area, (B and F) correlate to the hinge area, (C and G) correlate to the post-hinge area and (D and H) correlate to the LMM. (Singh et al., 2017)

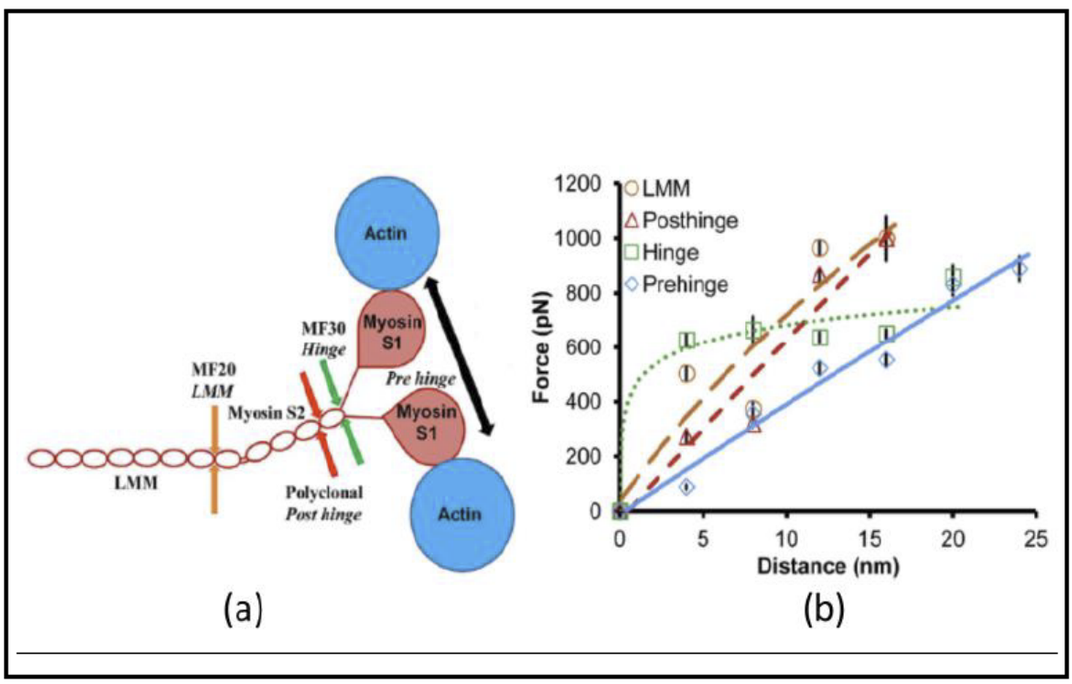

Figure 3.2: Pulling sites on myosin and the force required in SFS. (a) Shows the 4 pulling sites on myosin: pre-hinge black arrow, hinge green arrow, S2 red arrow and LMM orange arrow. (b) The pre-hinge (blue), hinge (green) and post-hinge (red) required less force to pull than LMM (orange).(Singh et al., 2017)

3.2 Stabilizer Design and Its Effect on the E930del Myosin

The stabilizer was designed to wrap around myosin S2 and stabilize it. It is made of a stretch of polylysine amino acids with few substitutions to allow it to bend and wrap around part of myosin S2. Due to its positive charge content, the stabilizer is expected to form stronger bonds around longer strips of negative charges. One such strip (927-931) is in the S2 region of myosin as shown in Fig. 3.3, where the blue colored residues represent the positively charged amino acids while the red colored residues are the negative amino acid.

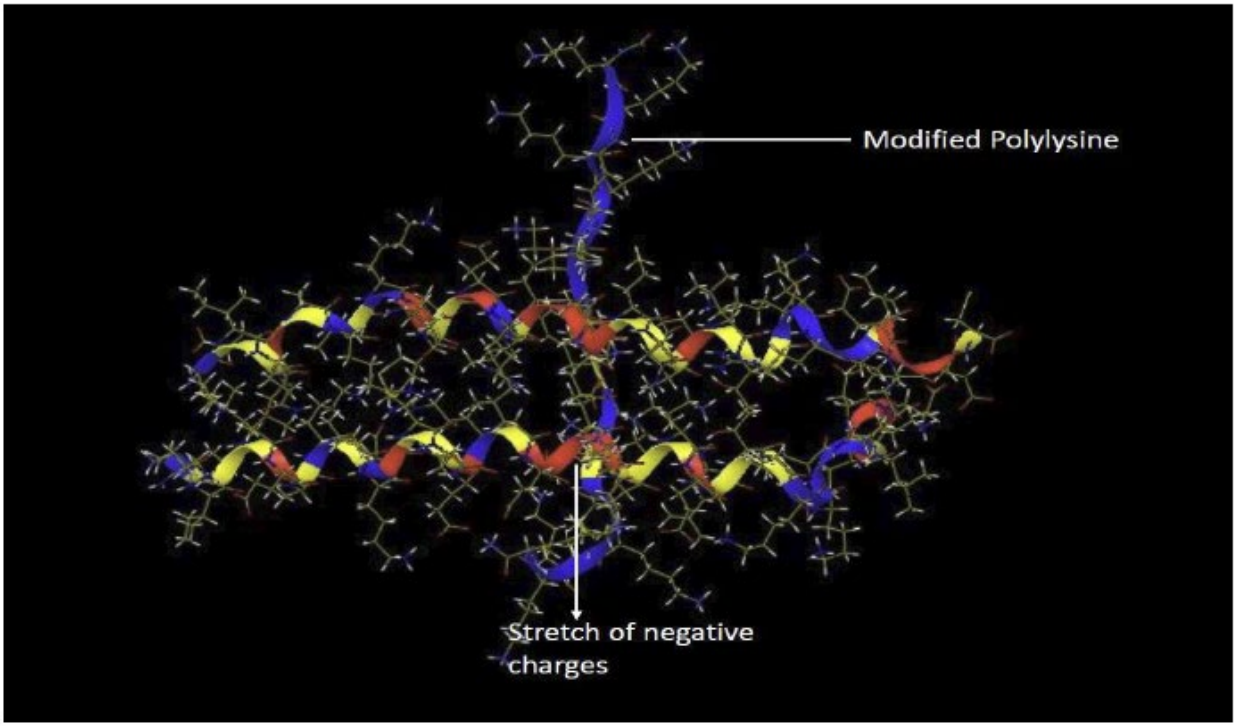

Figure 3.3: Computer simulation modeling for the binding of the stabilizer with WT myosin. The stoichiometry was measured to be 1 stabilizer to 1 WT myosin dimer; however, the stoichiometry was 2 stabilizers to 1 myosin dimer in the E930del mutation as revealed by the anisotropy results (unpublished data).

SFS was used to determine the optimal stabilizer length to hold the E930del together. By comparing 12, 17 and 21 a.a. stabilizer lengths (Fig. 3.4 and Table 3.1) interacting with E930del myosin, the 17 a.a. length stabilizer showed the most promising

results in accordance with the ELISA tests (unpublished data). The integration of the SFS force spectrum, which represents the force required to separate the E930del myosin dimer, was 36,486 kJ in the presence of the stabilizer compared to 4,205 kJ for E930del myosin alone.

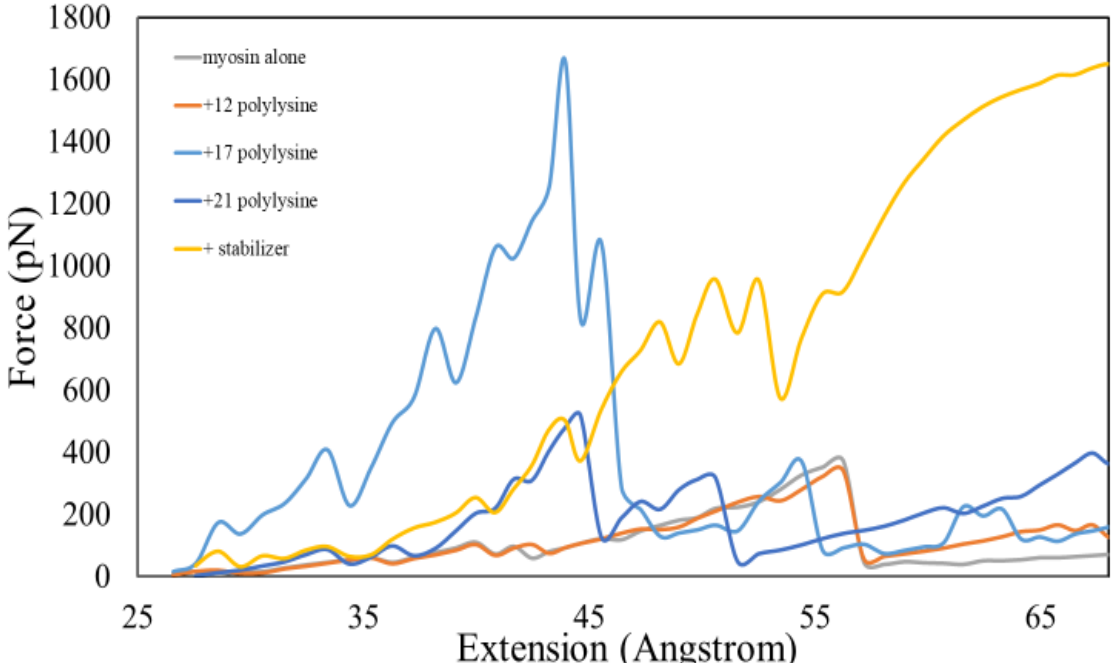

Figure 3.4: SFS traces for different polylysine lengths interacting with E930del mutation. The 17 polylysine and stabilizer provided the highest stability for the E930del compared to other polylysine lengths according to the SFS traces. Table 3.1 shows the integrated forces which reached 9 folds in some instances.

Table 3.1: Force integration from SFS for E930del, E930del with 12 a.a., 17a.a. and 21 a.a. polylysine and E930del with stabilizer. Highest force was for the 17 a.a. length polylysine and stabilizer.

Myosin type	Force spectrum (kJ)
E930del	4,205
E930del with 12 polylysine	7265.78
E930del with 21 polylysine	13049.8
E930del with 17 a.a. polylysine	24,370
E930del with stabilizer	36,486

In dynamic simulation, where the molecules were allowed to interact freely in the solution at 310 K for 16ns, the WT myosin dimer remained intact as shown in the upper panel of Fig. 3.5, while the E930del separated as shown in the middle panel, however; the E930del regained the WT property and remained attached after the addition of the stabilizer as shown in the lower panel. The helical content, which represents the retrieval of the WT properties, was also measured for the structures that came out from dynamic simulation using Ramachandran plot over the simulation period. As shown in Fig. 3.6, the WT showed a little below 85% helical content by the end of the simulation period, while the E930del showed descent in the helical content to below 70%. The helical content was recovered to above 85% when the stabilizer was added to the mutated E930del myosin, suggesting high efficiency in stabilizing the mutation.

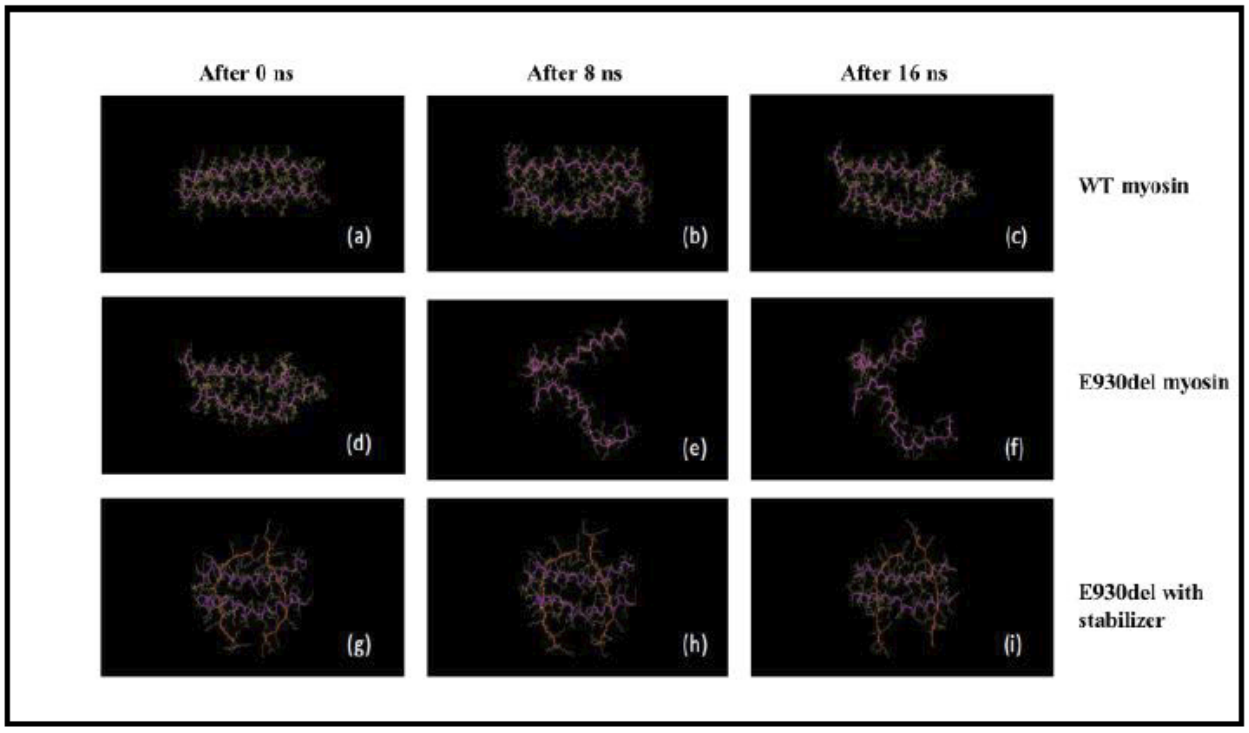

Figure 3.5: Dynamic simulation for 35 a.a. of WT myosin, E930del myosin and E930del myosin with stabilizer over 16 ns. Three snapshots were taken at the beginning of the simulation, after 8 ns and after 16 ns. The wild type kept its integrity while the E930del broke apart, then the E930del regained its WT integrity upon the addition of the stabilizer.

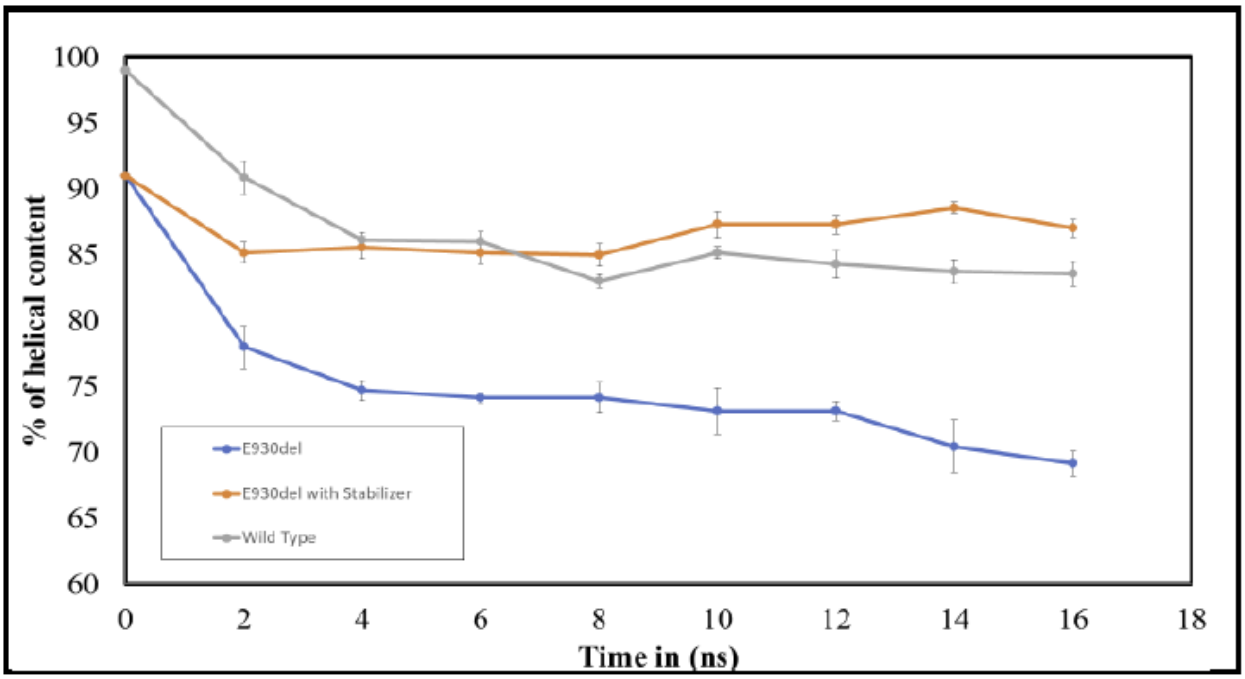

Figure 3.6: Helical content in myosin after dynamic simulation. The E930del had the lowest helical content, while the WT myosin had higher helical content. The E930del mutation regained its WT property with high helical content upon the addition of the stabilizer.

3.3 Destabilizer Design and Interaction with Myosin

Computational chemistry was used to design the destabilizer by targeting the major amino acids that contribute to the S2 stability. SFS measurements were run on WT myosin as shown in Fig. 3.7. Two pairs of amino acid attachments were determined to contribute -at least partly- to the stability of the S2, with the rest of the stability contributed mainly through the heptad repeat, which induces the hydrophobic amino acids of the myosin to come together, while the charged amino acids to form electrostatic forces. The 2 pairs of amino acids that were found to contribute to the stability of the S2 region mostly were E-R and E-N, which have peaks extending from 62 A^o to 111 A^o, reaching to a force of 700 pN in some instances (Fig. 3.7). These amino acids were targeted to break the myosin dimer strong attachment.

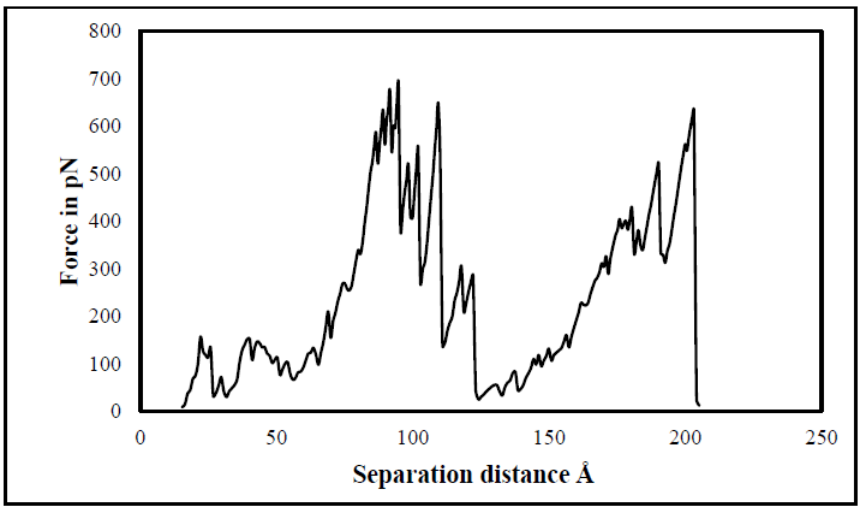

Figure 3.7: SFS for a 19 a.a. (921-939) WT peptide of the S2 region. The 85 Aº peak separation distance represented the E930-R925 amino acid pair and the 108 Aº peak represented the N929-E933 amino acid pair.

The destabilizer design process involved testing several candidates; each with different amino acid substitutions to determine the one with the highest interaction energy with S2. One candidate had an interaction energy of -262 kJ compared to -82 kJ (Table 3.1) for the WT myosin dimer, almost 3 times the bond strength. This candidate is proposed to interact with S2 as shown in (Fig. 3.8). It is thought to interpose between the S2 dimer molecules as they unwrap with each contraction in a process called “breathing”, allowing the exposed S2 to bind to different molecules.

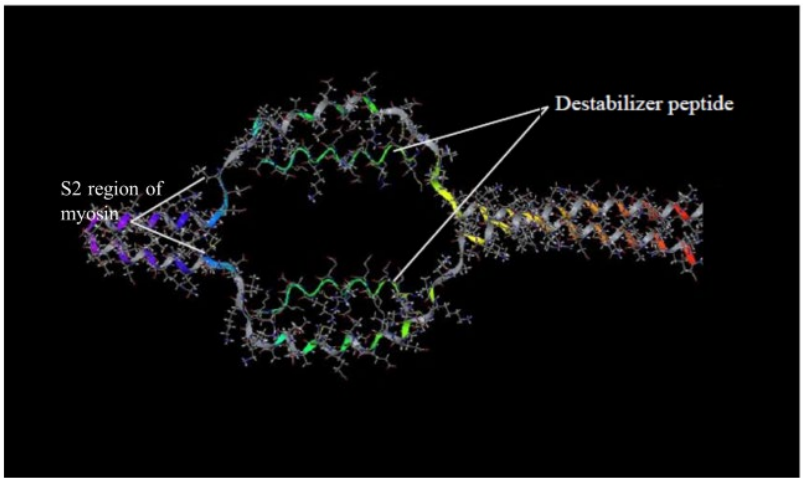

Figure 3.8: The destabilizer was designed to compete with myosin dimer formation.

3.4 Discussion and Conclusion

Several reports have suggested that S2 is a flexible domain in myosin (Li Y et al., 2003, Blankenfeldt et al., 2006) and has a potential role other than being a linker between the head and the tail. Its role in contraction was proposed after correlating several mutations that cause hypertrophic cardiomyopathy to that region. Further examination of the mutations that cause HCM revealed that they induce the S2 to become less stable, therefore, a possible correlation between S2 flexibility and its role in contraction was brought forward. In the work presented here, (SFS) was used to determine the stability of the S2 by comparing it to different myosin sites: the head (N-terminal region), S1-S2 hinge, S2 and LMM. As expected, the LMM showed more rigidity in pulling compared to other parts of myosin, while the S2 was easier to unwrap. This result comes in correlation with the Gravitational Force Spectroscopy (GFS) experiments (Singh 2017), where antibodies that attach to different sites on myosin were used to pull myosin strands apart using the gravitational force. It was found that the S2 required less force to unwrap compared to the LMM. This funneled in the same stream of research that proposed higher than normal S2 flexibility.

FHCM disease was tackled in this research by designing a molecule that has the potential to stabilize the mutated hyperflexible S2 region. After closely studying S2 mutations, it was found that there was high content of negatively charged amino acids, hence came the idea of designing positively charged molecule. Several amino acid substitutions were introduced to induce a bend in the structure to allow it to wrap around the myosin. SFS showed that the 17 amino acid long structure had the best results. It increased the stability of the E930del mutation 9 times from 4,205 kJ to 36,486 kJ.

Molecular dynamics showed that the stabilizer held the mutated E930del together, unlike E930del alone which separated after 16 ns. The helicity content of the E930del was partially lost due to the mutation, but the stabilizer retrieved that with a helicity content of 85%, alomst similar to the WT helicity content.

Based on the same concept of S2 stability modulation, another molecule was built with the purpose of increasing contractions, it was called the destabilizer. This molecule was designed to target the S2 region of hypocontractile hearts to further destabilize it and prevent it from dimerization. The design was based on WT myosin S2 SFS simulations to determine the major amino acids that contributed to S2 stability so they could be targeted. The novel destabilizer construct exhibited three-fold interaction energy increment over the myosin dimer with -228 kJ for the destabilizer compared to -82 kJ for WT myosin.

In conclusion, further evidence to S2 instability was provided through computational chemistry tests. Then the instability concept was utilized in building the stabilizer peptide to decrease contractions, and it was also adopted to increase contractions through the destabilizer model.

CHAPTER 4

HEART HOMING ADDUCTS AND MASS SPECTROSCOPY

4.1 The Search for Heart Homing Adducts

The search for a suitable heart homing adduct was laborious as the literature had several potential candidates. Table 4.1 lists some heart homing peptides (HHP) and adducts, where APWHLSSQYSRT and CRPPR showed high potential among the homing peptides with an interaction energy of -234 kJ for APWHLSSQYSRT and -276 kJ for CRPPR. Since APWHLSSQYSRT was highly cited in the literature, it was chosen over CRPPR, but due to the irreverable nature of the bond between the HHP and the anti-myosin S2 peptides, there was a concern that the HHP might not be cleaved inside the cell, which may affect the anti-myosin S2 peptides functionality.

Table 4.1: Interaction energy of WT human S2 with different heart homing peptides and adducts that were attached to the destabilizer. The destabilizer with CRPPR showed the highest interaction energy for the HHP and the destabilizer with TA showed the same high energy for the heart adducts.

Heart homing peptide	Interaction energy (kJ)
WT S2	-82
Destabilizer	-228
Destabilizer with CRPPR	-276
Destabilizer with APWHLSSQYSRT	-234
Destabilizer with KSTRKS	-200
Destabilizer with CRKDKC	-193
Destabilizer with DDTRHWG	-192
Destabilizer with CARSKNKDC	-190
Destabilizer with TA	-276

Meanwhile, a paper came in the literature describing the strong potential of tannic acid (TA) in shuttling different proteins to the heart. According to the authors, several

proteins were attached to TA including GFP, viruses and some other peptides, and were all shown to be transported to the heart. It is expected that these proteins bind non-covalently to TA, or with an ester bond that could be broken inside the cell by esterases, reducing the potential for dirupting peptides' functions. Furthermore, TA reaction with peptides was quite simple, it required vigorous shaking for 3 days. Their interaction energy was also high (-276 kJ) as shown in Table 4.1. Thus TA represnted a suitable alterantive for the APWHLSSQYSRT.

4.2 TA-Destabilizer Mass Spectroscopy (TA-DE)

The bond between the TA and the peptides was further investigated with mass spectroscopy. The peak of interest should have three characteristics; first it should match the m/z for the TA-DE molecule, second it should show in the TA-peptide run only but not in the peptide alone or TA alone run and third it should be a consistent peak, that is, it should show in multiple runs. The search was not easy because there were many peaks that had to be analyzed a s several TA bonds broke during different mass spectroscopy runs.

The TA-DE was first run in water as shown in Fig. 4.1 but no TA-DE peak showed, suggesting specific buffer requirements for the reaction to occur. When the same reaction was run in PBS, the results came as shown in Fig. 4.2 where (a) shows 2 peaks for the destabilizer (581 and 775) that corresponded to the molecular weight of the destabilizer attached to 4 hydrogens ((2322+4)/4=581.5) and 3 hydrogens ((2322+3)/3=774.5) respectively. Fig. 4.2(b) shows TA spectrum fragmenting in strong ionization field leading to 659, 811, 963, 1115 and 1267 peaks (notice the 152 difference between the readings) which were interpreted as (Fu et al., 2019):

glucose + sodium + n X galloyl moieties + proton

(180 + 22 + nx152 + 1).

When the TA and the destabilizer were reacted together in PBS buffer at 1 mM TA : 0.1 mM DE as shown in Fig. 4.2(c) two new peaks (589.7 and 785.5) emerged and were not in the destabilizer alone or TA alone spectra. More importantly they corresponded to the binding between the TA and destabilizer. The peaks were interpreted as:

-DE + TA + 4xgalloyl – water + molecular weight of sodiums and/or potassiums + no. of protons) / no. of the protons

(2322 + 1700 + 4x152 - 18 + (23+(2x39)+ (6 or 8))/(6 or 8)= 589.75 if divided by 6, or 785.5 if divided by 8.

Table 4.2 has interpretations for the rest of the bonds.

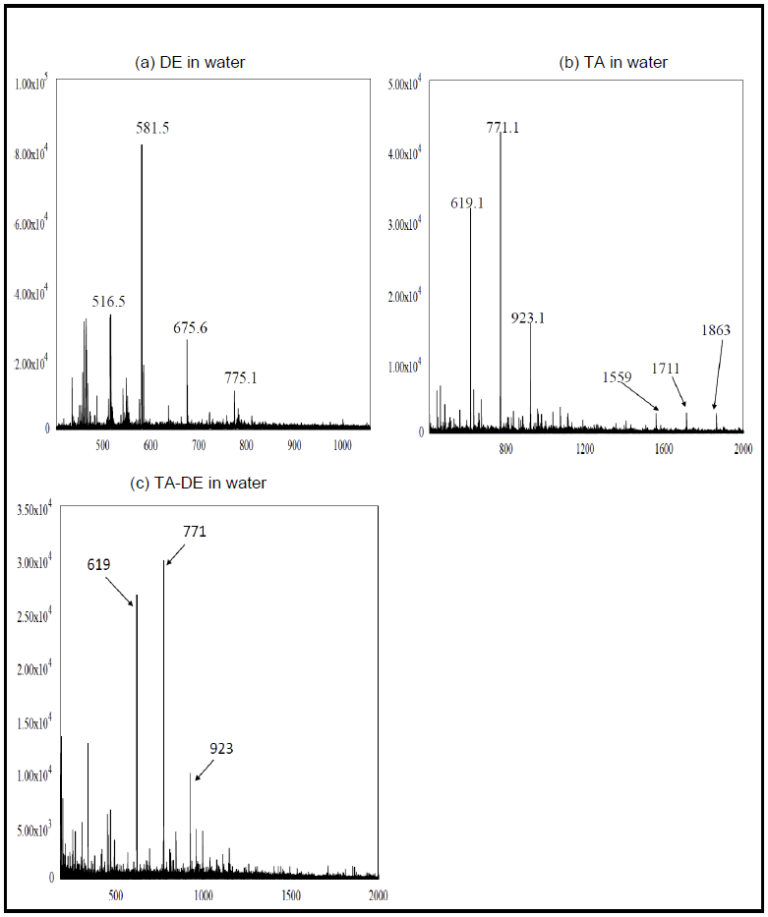

Figure 4.1: TA, destabilizer and TA-DE in water. (a) DE in water. (b) TA in water. (c) No TA-DE peak showed in water, suggesting special buffer requirements for the reaction.

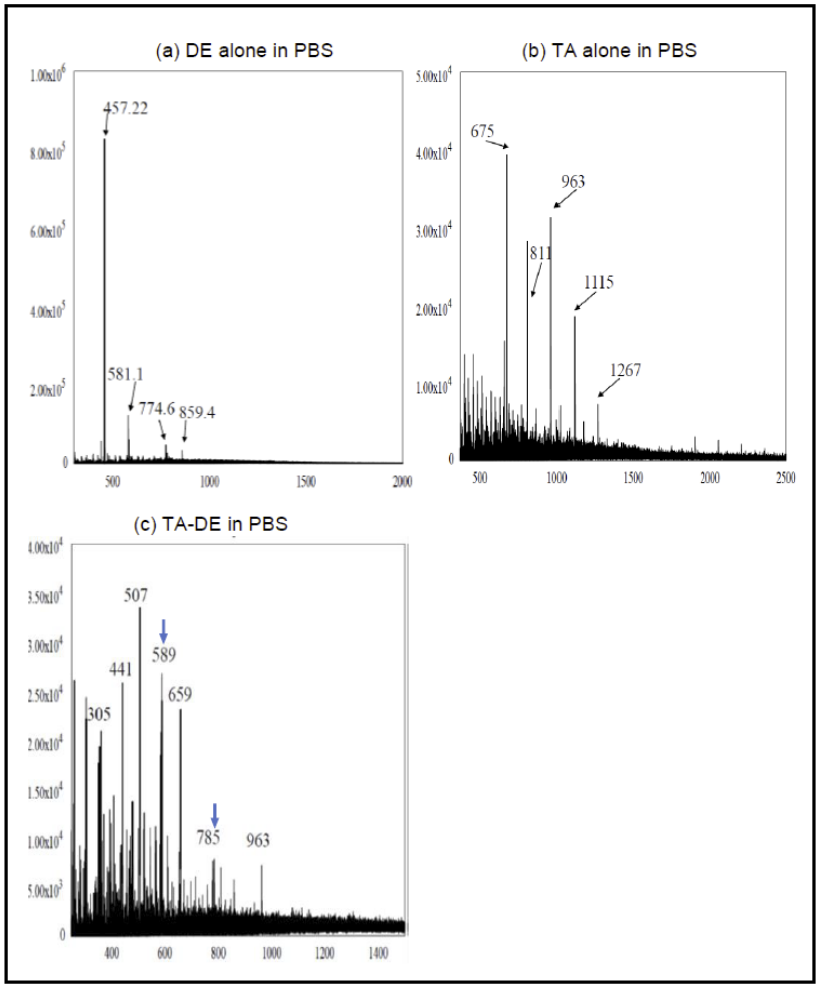

Figure 4.2: TA, Destabilizer and TA-DE in PBS. (a) DE alone in PBS. (b) TA alone in PBS. (c) The TA-DE run in PBS produced 589.75 and 785.5 peaks that corresponded to the TA-DE complex (they are marked with blue arrows).

Table 4.2: Interpretations of different peaks that showed in the mass spectroscopy runs: (a) stabilizer and destabilizer peaks (b) TA peaks and (c) TA-ST and TA-DE peaks

Peaks (m/z)	Interpretation
(a) Molecular species of stabilizer and destabilizer detected by mass spectroscopy	
582, 775	(destabilizer + n x protons)/n (2322 + n)/n
516	(2 x destabilizer + 9 x protons)/9 (2x2322 + 9)/9
432, 540, 720	(stabilizer + n x protons)/n (2158 + n)/n
564, 677, 753	(3 x stabilizer + 3 x phosphate + n x protons)/n (3x2158 + 3x98 + n)/n

Peaks (m/z)	Interpretation
(b) Molecular species of TA detected by mass spectroscopy	
1903, 2055, 2207	2xglucose + sodium + nxgalloyl moieties + 1xproton 2x180 + 22 + nx152 + 1
5155	(water + glucose + 10xgalloyl moieties) x 3 + 1xproton (18 + 180 + 10x152) x 3 +1
355, 507, 659, 811, 963, 1115, 1267	glucose + sodium + nxgalloyl moieties + proton 180 + 22 + nx152 + 1
619, 771, 923	glucose-water+proton+galloyl moeities 180 - 18 + 1 + nx152
1559, 1711, 1863	2xglucose-water+proton+galloyl moeities 2x180 - 18 + 1 + nx152
502, 654, 806, 958, 1110, 1262, 1414	Glucose+ gallic acid+proton+galloyl moieties 180 + 170 + 1 + nx152
1594, 1898, 2050, 2201, 2353	glucose+2Xsodium+proton+galloyl moieties 2x180 + 2X22 + 1 + nx152
(c) Molecular species of TA-ST and TA-DE detected by mass spectroscopy	
409	Stabilizer + 1 glucose + 3 X galloyl moieties + 2 X potassium + 7 -18) / 7 -(2158 + 180 + 3x152 + 2x38 + 7 -18)/7
589, 673, 785	DE + TA + 4xgalloyl – water + molecular weight of sodiums and/or potassiums + 8,7 or 6 protons)/ 8,7 or 6 no. of protons (2322 + 1700 + 4x152 - 18 + (22+(2x38)+ (8,7 or 6))/(8,7 or 6)

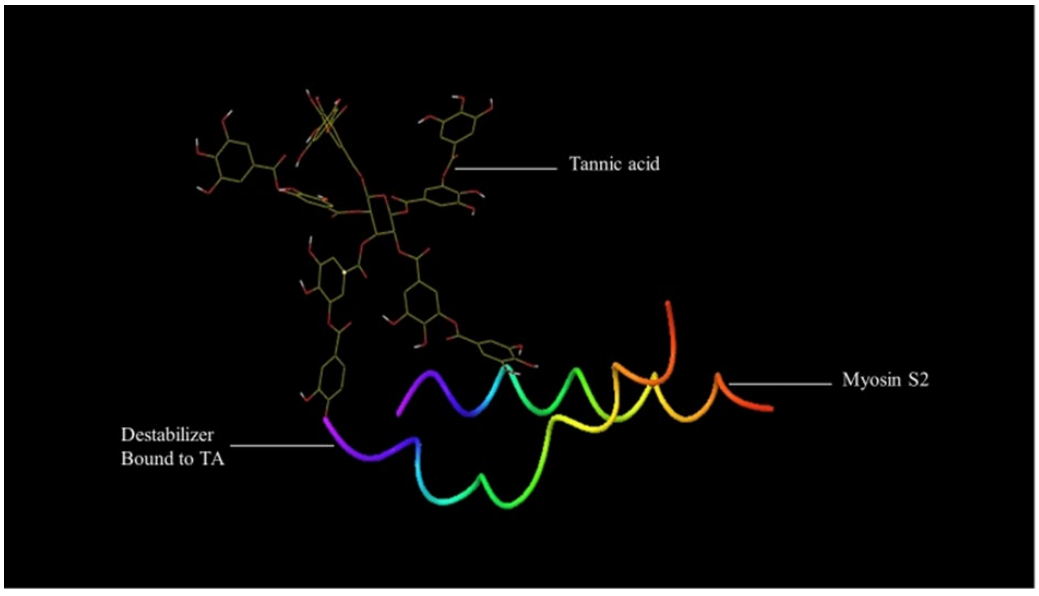

Figure 4.3: TA esterified to the destabilizer. The same mechanism is thought to govern the ST-TA attachment. The DE-TA complex is non-covalently bound to the myosin S2.

The 589.7 peak was more consistent than the 785.5. However, they both support the esterification of the destabilizer to TA in a covalent manner after long incubation period, which involved dehydration reaction that was detected by the loss of 18 daltons (Fig. 4.3). This bond could possibly be broken inside the cells by the activity of the intrinsic esterases.

4.3 Purification of Extra TA from TA - Anti-Myosin S2 Peptides

To prepare the TA-anti-myosin S2 peptide complex for animal model testing, the extra unbound TA was purified from the TA-anti-myosin S2 peptide complex for the potential toxicity of TA on animals. A protocol that could be easily deployed to any location was prepared since the animal model tests will be performed off campus. To this end, a G-10 column, 3 inches in length and three quarters of an inch in diameter was prepared.

To determine the peptide content in the elution after the purification step, Bicinchoninic acid (BCA) assay and fluorescamine assay were employed. Both methods are used to measure protein concentration at small scale. In BCA assay, all tubes turned dark purple without being discernible. It seems that there was interference from TA. On the other hand, the fluorescamine assay was not affected by the presence of TA in the solution, therefore, it was the method of choice. The purification process was initiated by dispensing 250 µl of the sample containing 1 mM TA : 0.1 mM destabilizer on the column's top end. Then 1 ml of PBS buffer was serially added, and 0.5 ml fractions were manually collected. The extra TA precipitated during the preparation of the samples and was filtered by the column. As shown in Fig. 4.4, the peptides were concentrated mainly in tubes 3 and 4 according the fluorescamine assay. However, when these tubes were run in mass

spectroscopy (Fig. 4.5), TA peaks were dominant over TA-DE peaks, thus, it was required to think about another approach to eliminate the extra TA.

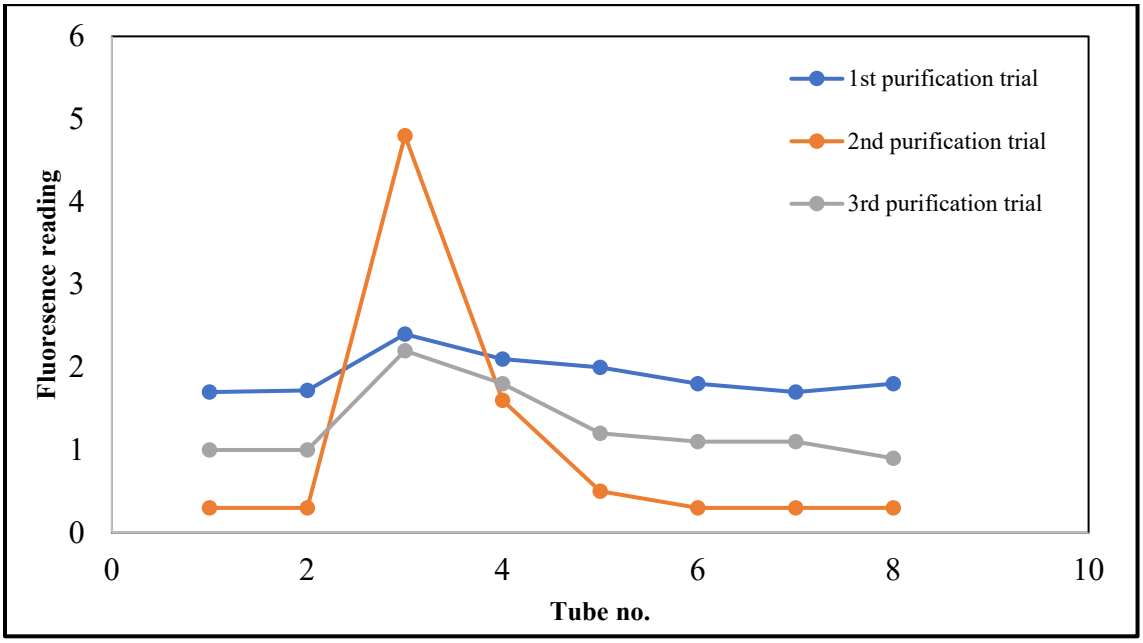

Figure 4.4: The relative amount of protein in the tubes according to the fluorescamine assay. Tubes 3 and 4 had the highest amount of proteins in all three trials.

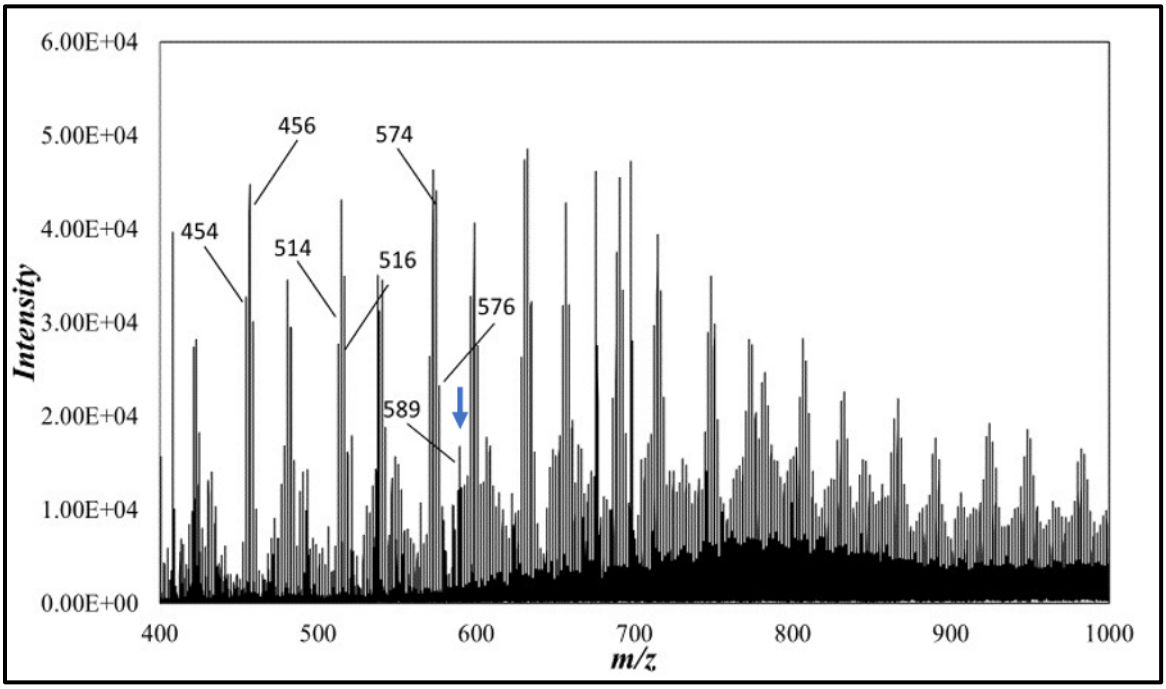

Figure 4.5: TA was still present at high concentrations after purification with G-10 column. All the peaks shown above belong to TA except the 589 peak which appears to correspond to DE-TA.

4.4 Reduced TA:DE Ratio

Since the purification step did not eliminate the extra unbound TA, it was imperative to take another route to reduce it, thus, TA starting concentration was reduced from 10X the concentration of the anti-myosin S2 peptides to 5X, then 1X . The results are illustrated in Fig. 4.6 from low DE concentration to high DE conentration: in (a and b) TA and DE were at concentrations 0.1 mM DE : 1 mM TA, in (c and d) the concentration was 0.1 : 0.5, in (e and f) it was 0.2 : 0.2, in (g and h) it was 1:1, in (i) The DE was run on its own at 0.2 mM concentration and in (j) the TA was run on its own at 1mM. All runs showed the expected TA-DE peaks at 589 and 785 except the 1:1 mM concentration. At this concentration the tubes became cloudy the moment the reactants were mixed together suggesting an interaction between the TA and DE despite not showing the expected 589 and 785 peaks. The peaks that showed in this run were considered -with high liklihood- to be TA-DE peaks. Two such peaks were the 581.5 and 585. A possible interpretation for these peaks as well as for other TA:DE peaks is in Table 4.2, where the equation that was used to solve for the numbers in the table is:

> DE + TA + 4xgalloyl – water + molecular weight of sodiums and/or potassiums + no. of protons)/ no. of the protons.

The 581.5 and 585 peaks came from:

> 2322 + 1700 + (4x152) - 18 + 39 + 8/8 = 581.5 and 2322 + 1700 + (4X152) - 18 + 39 + (23X2) + 8/8 = 585

However, the 581.5 peak that showed in the DE alone run in PBS Figs. 4.5(i) and 4.2(a) was interpreted as DE peak (Table 4.3). The interpretation is determined mainly by the reactants.

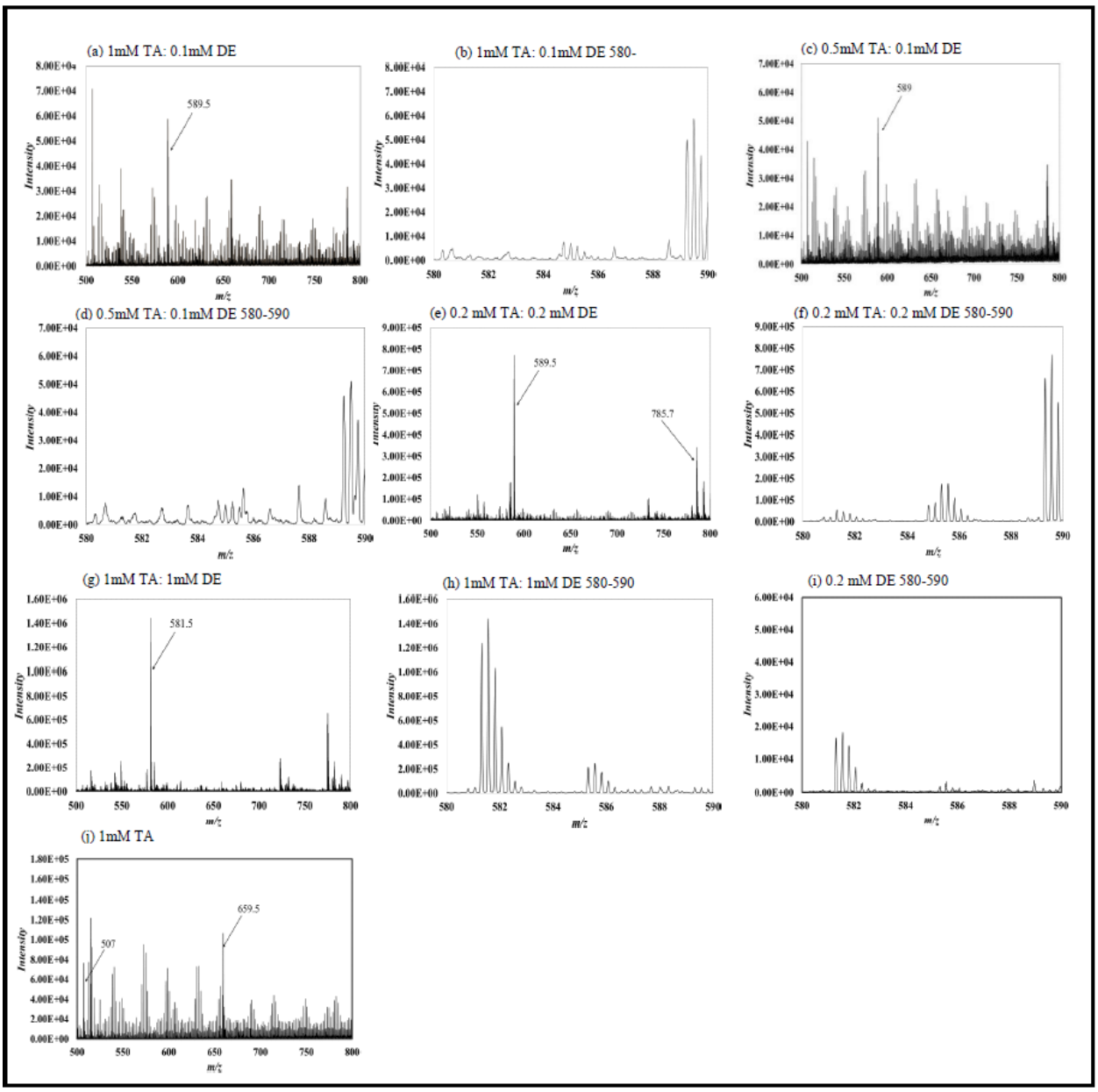

Figure 4.6: TA-DE peaks at lower TA:DE ratios. (a and b) 1 mM TA:0.1 mM DE, (c and d) 0.5 mM TA: 0.1 mM DE, and (e and f) 0.2 mM TA:0.2 mM DE showed the prominent TA-DE peaks (589.5 and 785). (g and h) 1 mM TA: 1 mM DE showed the 582 which is also described as TA-DE peak (see text). (i) showed the 582 peak that represents the destabilizer alone peak (see text). (j) showed the TA-alone prominent 507 and 659 peaks at 1 mM TA concentration.

The complex nature of the mass spectroscopy data made it hard to keep track of various peaks, therefore; they were featured in an easy-to-decipher plot in Fig. 4.6. In the plot, the 507 and 659 peaks represent TA- alone peaks that increase with increasing TA concentrations, however; at 1:1 mM concentration, these peaks decreased especially

when compared to the 1mM TA-alone runs, suggesting TA consumption due possibly to an interaction between TA and DE. The relative intensity dropped in peak 507 from 0.76 at concentration 1 mM TA: 0 mM DE to .51 at concentration 1 mM TA: 1 mM DE. It also dropped from almost 1 to 0.29 in peak 659 at the same conentrations. Several other TA peaks were seen in TA-alone runs, which might have decreased as well, but the 507 and 659 are the more common peaks. There was also an increase in the 582 and 585 peaks for the 1:1 mM concentration, which are thought to be TA-DE peaks as described earlier. The 1 mM TA : 0.1 mM DE, 0.5 mm TA : 0.1 mM DE and the 0.2 mM TA : 0.2 mM DE concentrations witnessed an increase in the 585, 589 and 785 peaks which are thought to be the more common TA-DE peaks.

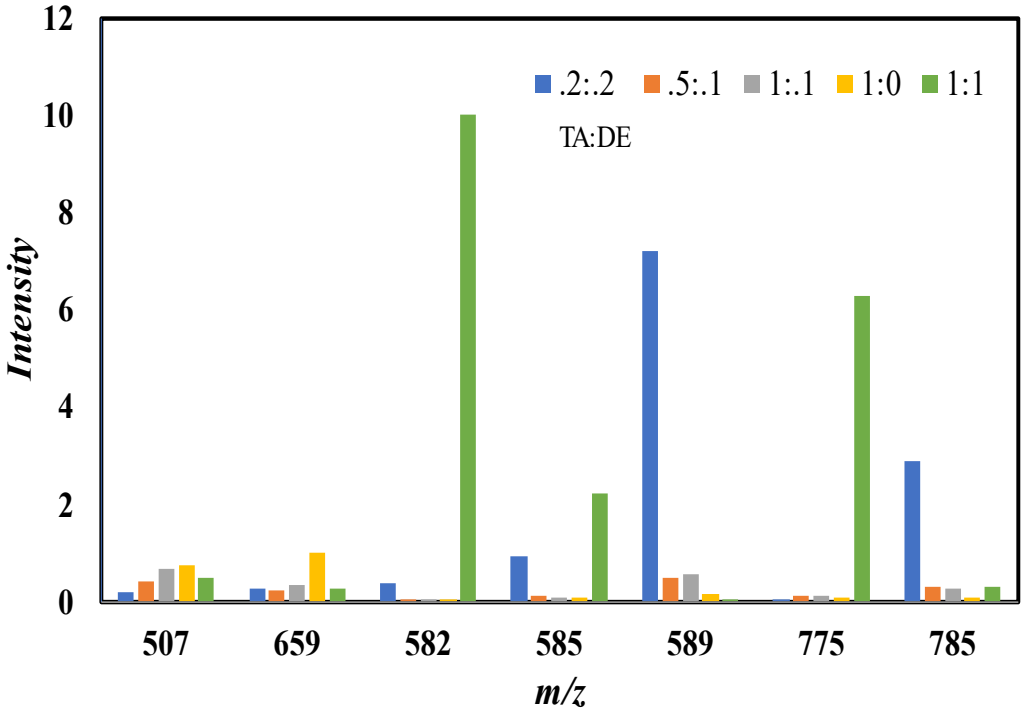

Figure 4.7: TA-DE and TA alone peaks summarized. The 507 and 659 peaks are TA peak; they increase with increasing TA concentration but decrease with high DE concentration suggesting a possible TA consumption due to TA : DE bond formation.

Table 4.3: Possible interpretations for the TA-DE peaks that showed at reduced TA:DE ratio. The equation that was used: DE + TA + 4xgalloyl – water + molecular weight of sodiums and/or potassiums+ no. of protons)/ no. of the protons.

Sodium	0	2	1	5	0
Potassium	1	1	2	0	3
8 protons	582.25	585	589.75	591.25	591.75
6 protons	776	779.6667	786	788	788.6667

4.5 TA-Stabilizer Mass Spectroscopy (TA-ST)

Similar to the TA-DE peaks, the TA-ST peaks should show only in the TA-ST spectrum and should be consistent. Therefore, these peaks would not be expected to show in the stabilizer alone runs. The peaks that showed in the stabilizer alone runs were as following [Fig. 4.8(a & b)]:

- The 432, 540 and 720 peaks, and were interpreted as:

  (stabilizer + n x protons)/n → (2158 + n)/n → (2158+(5,4 or 3)) / (5,4, or 3)

- The 564, 677 and 753 peaks, and were interpreted as:

  (3 x stabilizer + 3 x phosphate + n x protons)/n → (3x2158 + 3x98 + (9, 10 or 12)) / (9, 10 or 12).

  A detailed interpretation for the rest of the peaks can be found in Table 4.2(a).

- When TA alone was mixed in PBS [Figs. 4.2(b) and 4.8(c)] the peaks that showed up were:

  659, 811, 963, 1115 and 1267 peaks, which were interpreted above in the DE-TA section and in Table 4.3.

- When TA was shaken with the stabilizer for 3 days at 1 mM TA : 1 mM ST, a new peak that never showed in the TA alone or ST alone runs showed in this run. The peak was at 409 [Fig. 4.8(d)] and it was interpreted as following:

  Stabilizer + 1 glucose + 3 X galloyl moieties + 2 X potassium + 7 -18) / 7

-(2158 + 180 + 3x152 + 2x39 + 7 -18)/7 = 409

This interpretation suggests the presence of an ester bond, which is possibly the same mode of bonding as the DE-TA (see above), however, this type of assumption needs to be confirmed with 2D gel electrophoresis.

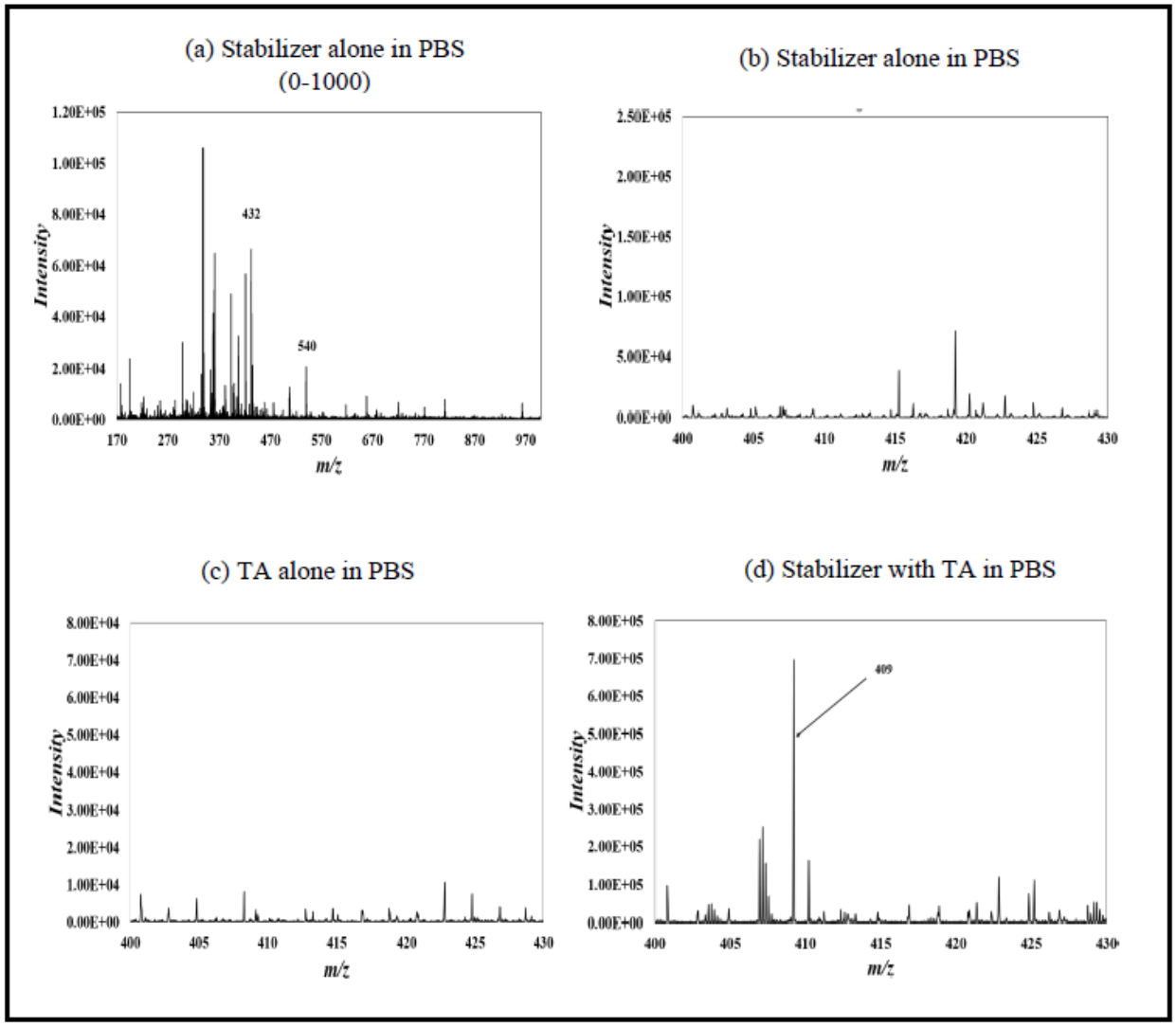

Figure 4.8: (a) Stabilizer in PBS (0-1000) (b) Stabilizer in PBS (400-430). (c) TA in PBS and (d) TA-ST is the only run that showed the TA-ST peak at 409 .

4.6 Discussion and Conclusion

The anti-myosin S2 peptides cannot target the heart on their own, hence the need for a heart homing adduct. Literature search in the heart homing peptides field led to

several candidates. These candidates were tested in our lab using computational chemistry which led to endorsing APWHLSSQYSRT sequence due to its high interaction energy (-234 kJ) and fair citations in the literature. Meanwhile, a research group reported the use of TA adduct to deliver various proteins and peptides to the heart. Fortunately, TA is widely available and has low toxicity, therefore, it was chosen as a heart homing adduct. Its reaction with peptides is quite simple requiring vigorous shaking for 3 days in PBS.

The bond between the destabilizer and the TA was confirmed using mass spectroscopy. It is believed to be an ester bond. To confirm its occurance, the destabilizer was run in PBS solution first, then TA was run by itself, then they were run together. New peaks at 589 and 785 showed only in the TA-DE spectrum but did not show in the destabilizer alone or TA alone runs.

TA is not very toxic, but to eliminate any possible toxicity, the TA-anti-myosin S2 peptide samples were run in size exclusion column G-10 to purify them from any unbound TA. However, the results were not promising as the samples still carried TA. Therefore, the strategy was changed to starting with lower proportion of TA-DE to reduce the unbound TA. Results from 0.5 mM TA : 0.1 mM DE run were promising and the 589.7 peak, which corresponded to the TA-DE bond, showed in the spectrum. The proportion was then further reduced to 0.2 mM TA : 0.2 mM DE and the TA-DE peaks were still predominant. At higher equimolar concentrations of TA and DE the tube was cloudy and little precipitation occurred. The peak that showed at these high concentrations was the 582 peak which was the same peak when the DE samples were run alone. The peak was interpreted in 2 alternative ways as follows:

In DE alone runs the 582 peak was interpreted as:

(2322 + 4)/4=582

In high concentrations of DE and TA, the 582 peak was interpreted as an ester bond between the TA and the DE:

(DE + TA + 4xgalloyl – water+ 1 potassium+ 8 protons)/ 8.

2322+1700+(4X152)-18+39+8/8=582.

By the same token, the TA-ST peak was confirmed using mass spectroscopy by running the stabilizer alone in the PBS solution first, then TA alone in PBS, then they were run together. A new peak showed at 409 only when TA and ST were run together. This peak corresponded to the TA-ST bond and it showed persistently in high amounts.

In conclusion, the anti-myosin S2 peptides were attached to TA as a heart homing adduct, and the bond was confirmed using mass spectroscopy.

CHAPTER 5

TA MINIMUM EFFECT ON ANTI-MYOSIN S2 PEPTIDES

5.1 Expansion Microscopy

This technique is known to enlarge samples 2-5 times their original size (Fig. 5.1). Here, expansion microscopy was used to determine whether TA affected the staining pattern of the sarcomeres or not. The samples were prepared by reacting TA with the fluorescently labelled anti-myosin S2 peptides by vigorous shaking for 3 days, then they were incubated with myofibrils for 3 days in the fridge before pursuing with the rest of the expansion microscopy preparation steps.

Myofibrils' staining of the C-zone with the fluorescently labelled peptides with and without TA [Fig. 5.2(a & b)] showed similar pattern. In both cases the destabilizer stained the C-zone weaker than the stabilizer because of the presence of MyBPC that is known to bind to the S2 region, which is the same region where the destabilizer binds, thus the destabilizer was excluded from binding to the C-zone. On the other hand, the stabilizer is less specific, thus it was able to bind to other parts of myosin in the C-zone and stain it brightly.

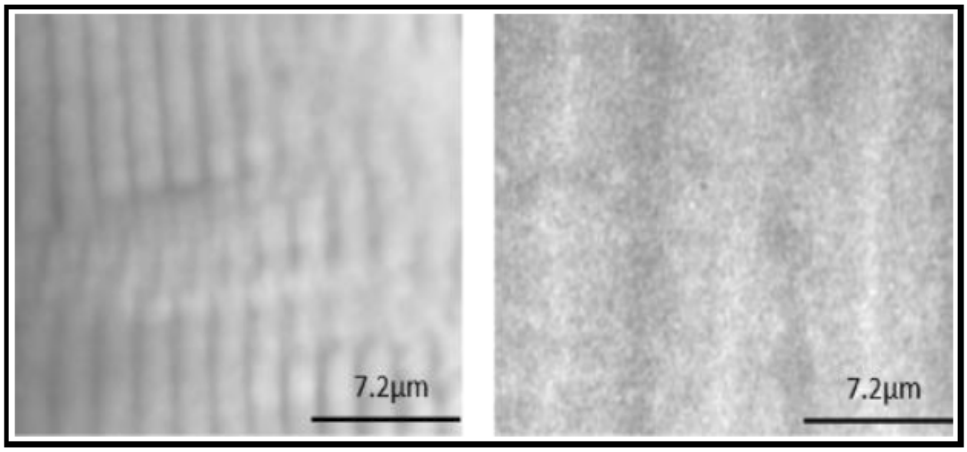

Figure 5.1: Expansion microscopy expands gels between 2-5 times. In this image the width of the sarcomere on the right spans the width of almost 4 sarcomeres on the left.

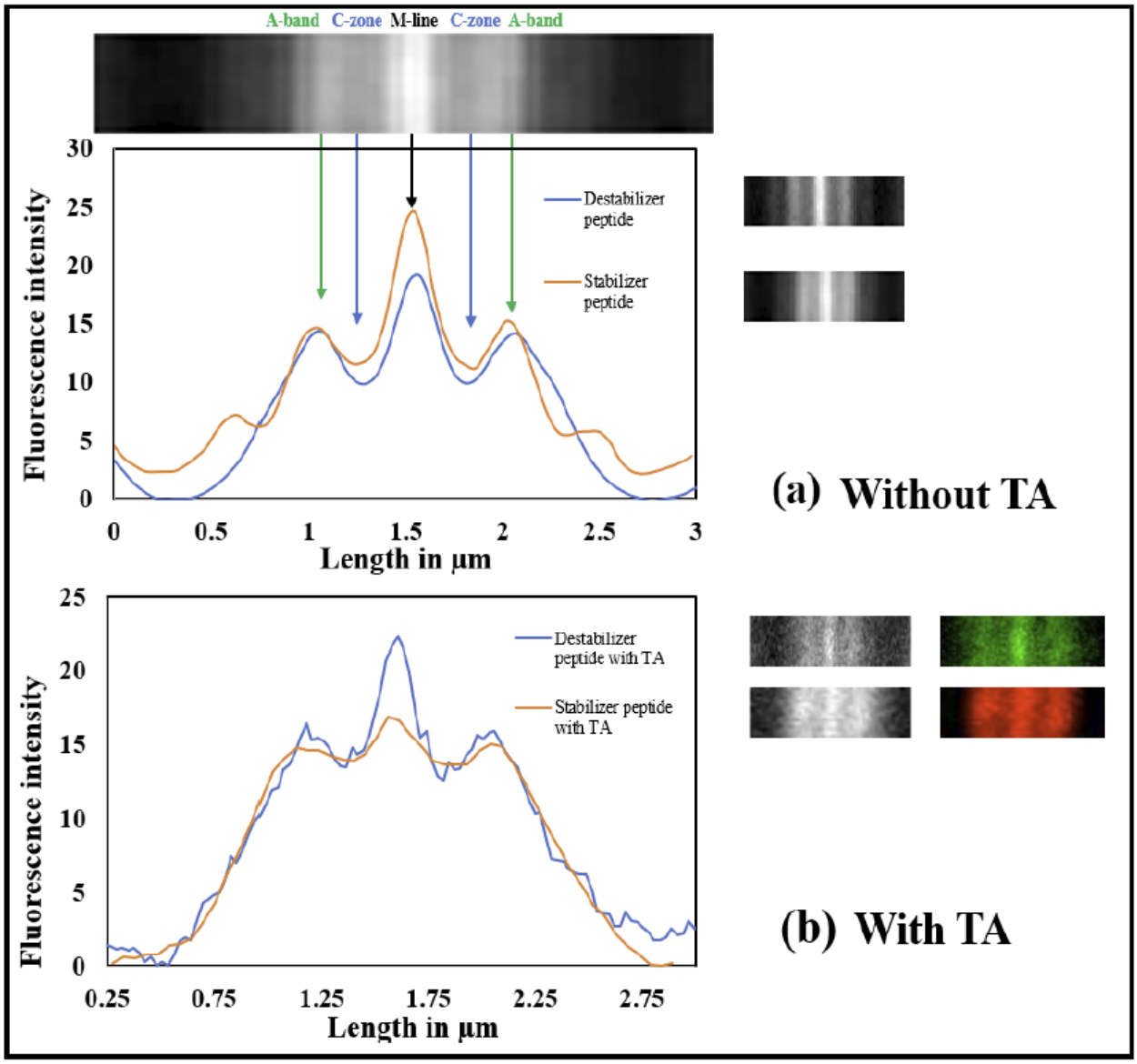

Figure 5.2: Comparing the staining pattern for the C-zone between the anti-myosin S2 peptides with and without TA. (a) The stabilizer showed more staining at the C-zone compared to the destabilizer. (b) The same pattern showed when TA was added to the anti-myosin S2 peptides where TA-ST showed stronger staining than the TA-DE. 100 sarcomeres were averaged in (a) while 15 sarcomeres were averaged in (b).

5.2 Contractility Assay

5.2.1 TA Alone Contractility Assay

It had been previously shown in our lab that the stabilizer and destabilizer tend to affect myofibrillar contraction (Singh, 2017). Nonetheless, it was essential to confirm that

their attachment to the TA did not interfere -or had minimum effect- on their interaction with myosin. To verify the effect of the TA on myosin, it was mixed alone with myofibrils at different concentrations. The results showed that its effect occurred at high concentrations around 10 μM and above where the contraction dropped from 16% to 13%, 10% and 6%, with concentrations of 0, 10, 100 and 143 μM of TA respectively as shown in Fig. 5.3.

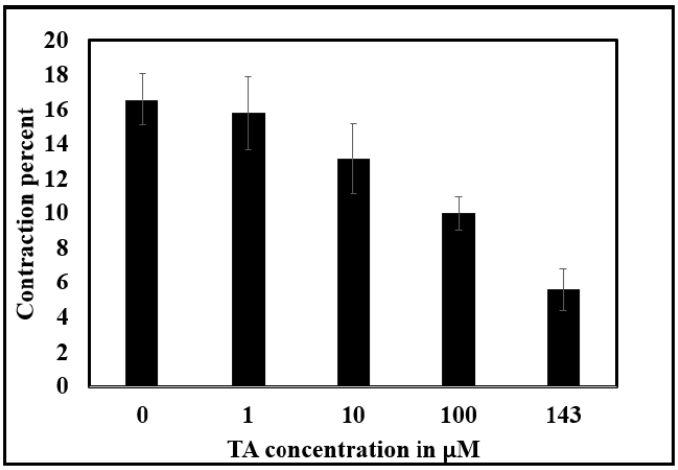

Figure 5.3: TA-alone effect on contraction. TA had minimum effect at concentrations below 10 μM but its effect became more prominent with higher concentrations of the TA reaching to contractions almost 6% with 143 μM concentration.

5.2.2 TA-Stabilizer Contractility Assay

TA showed minimum effect on the interaction between the stabilizer and the myosin as shown in Fig. 5.4. Kd for the stabilizer with myosin in the presence of TA was 3.37 ± 4.2 nM compared to 6 ± 1 nM in the absence of TA. Kd was measured using the equation

$$F(x)=17.5-((a*x)/(b+x)).$$

where F(x) is the contraction recorded (sarcomeric shortening) at different stabilizer concentrations, x is the concentration of the stabilizer, b is the Kd and plateau occurs at 17.5-a.

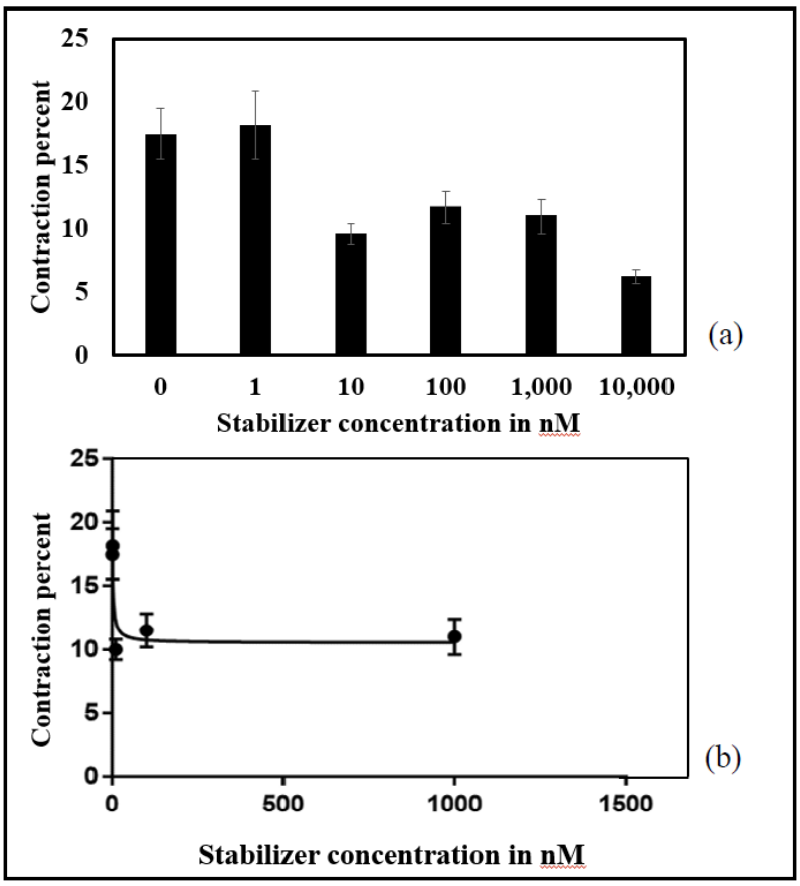

Figure 5.4: The effect of the TA on the stabilizer function through the contractility assay. The TA was mixed with the stabilizer at 10:1 concentration. The Kd of the TA-ST with myosin was 3.37 ± 4.2nM compared to 6 ± 1nM for the stabilizer alone suggesting that the TA barely had any effect on the stabilizer function.

5.2.3 TA-Destabilizer Contractility Assay

TA did not have significant effect on the destabilizer since the Kd for the destabilizer in the presence of TA was 1 ± 1 nM compared to 7.2 ± 2.7 nM in the absence of TA which is also considered minimal difference (Fig. 5.5). Kd was measured with the equation

$$F(x)=17.5-((a*x)/(b+x)).$$

where F(x) is the contraction recorded (sarcomeric shortening) at different destabilizer concentrations, x is the concentration of the destabilizer, b is the Kd and plateau occurs at 17.5-a.

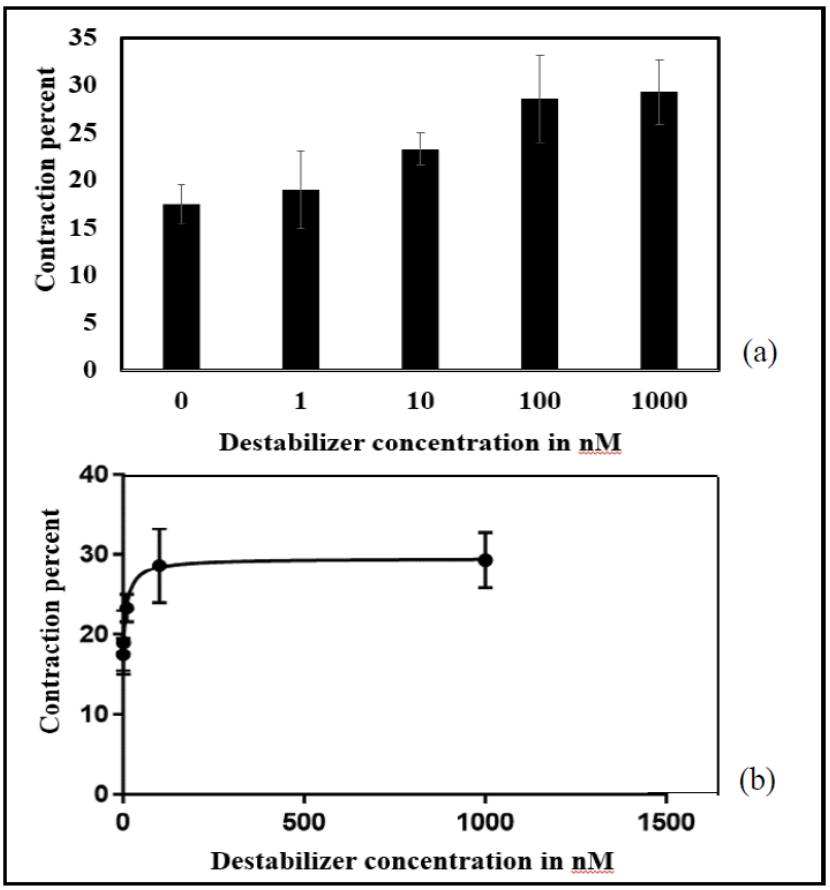

Figure 5.5: The effect of the TA on the destabilizer function through the contractility assay. TA was mixed with the destabilizer at 10:1 concentration. The Kd for the destabilizer with myosin in the presence of TA was 1 ± 1nM compared to 7.2 ± 2.7nM for the destabilizer alone.

5.3 Discussion and Conclusion

In this chapter, TA was tested for its possible influence on the anti-myosin S2 peptides functions through expansion microscopy and contractility assay. In expansion microscopy, the TA-anti-myosin S2 peptides were attached to fluorescent labels and reacted with myofibrils, then their positions were compared to anti-myosin S2 peptides alone. In the TA-ST case, the C-zone was bright, similar to the stabilizer alone pattern, while in the TA-DE case, the staining of the C-zone was darker, similar to the destabilizer alone pattern. This can be explained by the occupation of MyBPC to the C-zone and its strong affinity to the S2 region which excluded the destabilizer from binding, since the

destabilizer is specific to the S2 region only. This contrasts with the stabilizer case, where the C-zone was brighter due to the unspecific binding of the stabilizer.

In contractility assay, TA-anti-myosin S2 peptides were incubated with myofibrils and their contraction was compared to anti-myosin S2 peptides without TA. The Kd for the TA-ST complex was 3.37 ± 4.2nM compared to 6 ± 1nM for the stabilizer alone, while the Kd for the TA-DE complex was 1 ± 1nM compared to 7.2 ± 2.7nM for the destabilizer alone. These results suggested that the addition of the TA did not impact the anti-myosin S2 functionality.

In conclusion, TA did not seem to affect the anti-myosin S2 peptides functions with regard to position or contraction. This was confirmed through the expansion microscopy assay and the contractility assay, respectively.

CHAPTER 6

DISCUSSION AND CONCLUSION

6.1 Discussion

Figure 6.1 shows a schematic summary of the dissertation research. It had been assumed that myosin S2 is merely a linker between the myosin head and its tail. Later however several hypertrophic cardiomyopathy mutations were linked to that area especially the E930del (Richard et al., 2003) and E927del (Waldmuller et al., 2016). Further research concluded that it is highly likely that S2 plays a role in contraction. One hypothesis states that S2 instability may allow the heads to reach to actin and initiate contraction (Gundapenini et al., 2005). Another hypothesis suggested that the instable S2 region reduces the likelihood of folding the myosin heads back on the S2, which allows them to spend more time in the “on state” where they are ready to bind to actin. They are “turned off” however when MyBPC bends them on myosin S2 and blocks them from participating in contraction (Alamo et al. 2008 and Spudich 2015). In our lab, S2 instability was tested using computational chemistry by comparing the force required to pull different parts of myosin. It was concluded that S2 required the least force to pull apart. This result was further confirmed by GFS tests in our lab (Singh, 2017).

The immense instability of the S2 region in some FHCM mutations instigated us to think about a molecule to stabilize that region, thus came the stabilizer model. This molecule was designed with high incident of positively charged amino acids to bind to the negatively charged stretches of myosin. One such stretch -it is the longest- is in the S2 region, which may partly contribute to the instability of the S2 due to the repulsive forces of the counter monomer.

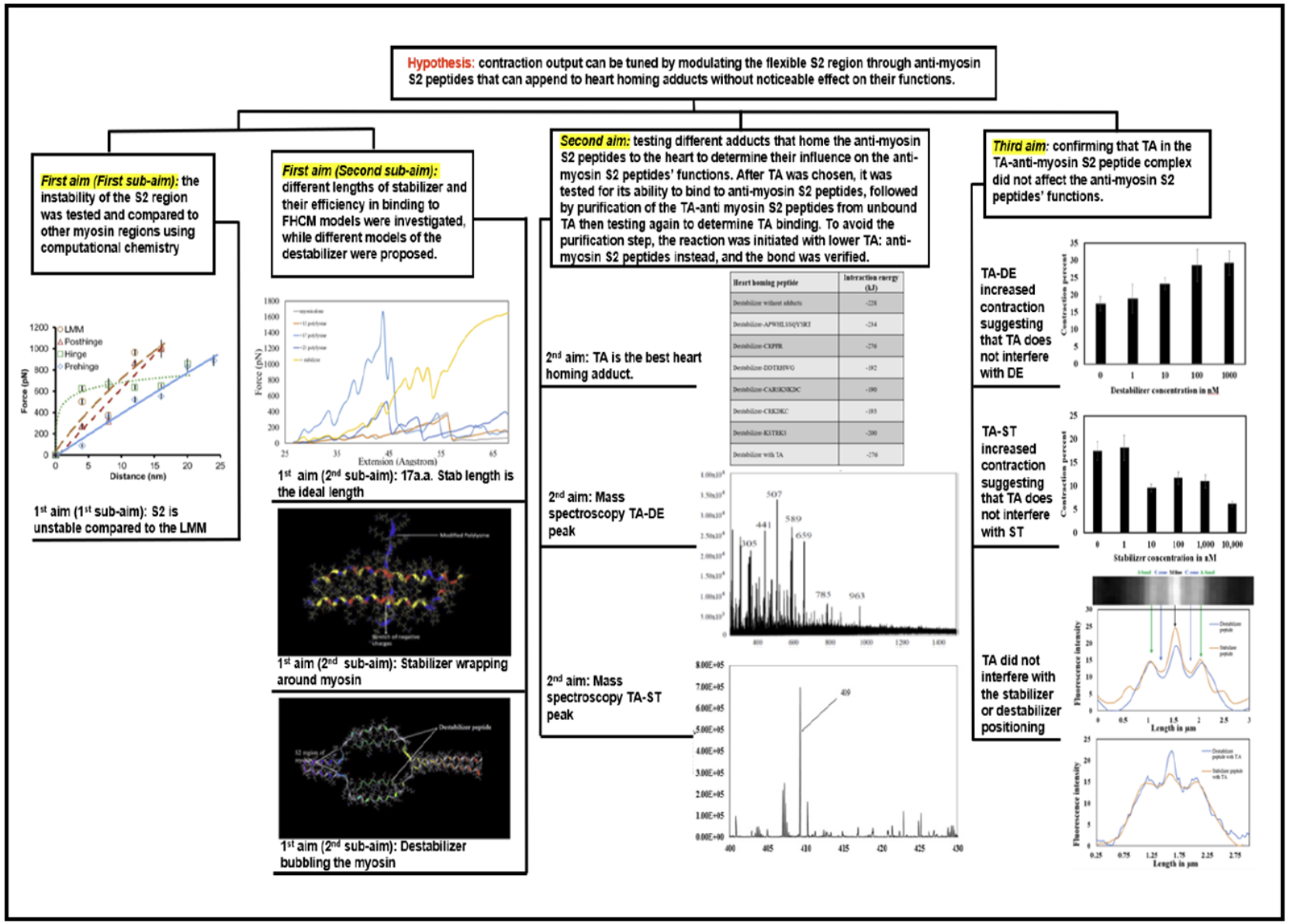

Figure 6.1: Schematic summary of dissertation research.

Computer mechanics simulation showed that the first make of the stabilizer binds to myosin S2 without being able to wrap around it. Some changes to the stabilizer sequence were made to introduce some kinks to allow it to wrap around myosin. Different lengths of the stabilizer were tested to determine the one with best length. Both ELISA and computational chemistry determined that the 17 a.a. length was the ideal length for the stabilizer to wrap and stabilize the myosin. Anisotropy results determined one stabilizer was required to wrap around WT myosin while 2 stabilizers were required to wrap around the E930del to stabilize it. SFS showed that the force required to unzip E930del was almost 9 times less than the force required to unzip the E930del with a well-wrapped stabilizer. Dynamic simulation, which simulates molecules over time, and includes the temperature factor, showed that the WT myosin dimer remained attached for the whole period of simulation and had a helicity content of 85% using the Ramachandran plot. These results opposed the results from the E930del which almost completely unzipped after 16ns of simulation and had a helicity content of almost 65%. When the stabilizer was added to the E930del at the beginning of the simulation, the myosin dimer remained attached to each other and had 88% helicity content, suggesting a stabilizing effect prompted by the stabilizer.

On the other hand, a molecule with the purpose of alleviating the symptoms of weakened hearts resulting from dilated cardiomyopathy or heart failure from heart attacks was also developed in the lab. The idea was based on MF30 antibody that is raised against one of the myosin S2 monomers and can destabilize it leading to higher contractions. Utilizing the same concept, the destabilizer was designed to destabilize the S2 region by outcompeting the myosin dimer formation. The design was based on S2

sequence with few amino acid substitutions to some residues that hold the S2 together to allow a stronger binding between the destabilizer and the complement monomer. The residues were determined with SFS as peaks requiring high forces to separate. After the design was built, the efficacy of the destabilizer (and the stabilizer) were assessed using several assays (Singh, 2017; Aboonasrshiraz 2020) including: GFS assay; which showed that myosin was harder to unzip in the presence of the stabilizer, and was more flexible in the presence of the destabilizer, the in vitro motility assay; where actin exhibited slower speeds when myosin was treated with the stabilizer compared to higher speeds of actin with the destabilizer, FRET assay; which showed high signal from the acceptor strand of myosin and weak signal from the donor strand when they were treated with the stabilizer because it brought them close enough for the energy to transfer, unlike the case when the destabilizer was examined, which caused the myosin to separate and halt the energy transfer. And several other assays that cannot all be mentioned here.

Interestingly, both the symptoms of hypertrophic cardiomyopathy and dilated cardiomyopathy have been managed by medical practitioners using the same types of drugs, for example: Angiotensin converting enzyme (ACE) inhibitors, which prevent the body from producing Angiotensin 2, a compound that is known to constrict blood vessels leading to an increase in blood pressure and heart load (Messerli et al., 2018), have been administered to counteract both HCM and DCM by dilating blood vessels to reduce friction. Beta blockers have also been used to control heart failures by blocking epinephrine (adrenaline) and norepineohrine neurohormones that increase the heart pace. Other potential drugs that are more specific to HCM and still in the animal model phase or have reached clinical trials are: Blebbistatin which is a myosin inhibitor that

prevents the actin and myosin from reacting together (Baudenbacher et al., 2008), Parvalbumin which has the ability to buffer calcium inside muscle cells (Couto et al., 2014), and MYK-461 that inhibits myosin ATPase (Hector et al., 2015). Mavacamten, which is currently in the more advanced stages of the clinical trials, works as an allosteric myosin modulator that inhibits the ATPase activity of myosin (Green et al., 2016; Rhode et al., 2018)) to reduce the number of myosin heads that participate in contraction. On the other hand, Omecamtive Mecarbil is a drug that is specific to DCM patients and showed high potential in clinical trials. The drug works by increasing the rate of ATP hydrolysis to ADP and Pi which allows myosin heads to attach faster and in greater numbers to actin during each contraction (Malik et al., 2011), thus possibly increasing contractions and alleviating symptoms of heart failures that may result from heart attacks and high blood pressure. The stabilizer and destabilizer may mimic these two drugs by being specific to HCM and DCM that cause increased and decreased ejection fraction respectively, but they have different mechanisms of actions.

The stabilizer and destabilizer (anti-myosin S2 peptides) may not be heart specific, therefore, a search for molecules (heart homing adducts) that would facilitate the entrance of the modifying peptides into the heart cells was commenced. Several adducts from the literature were tested using SFS to determine whether they had any impact on the interaction of the anti-myosin S2 peptides with myosin. APWHLSSQYSRT was picked as a heart homing peptide (HHP) for its interaction energy with myosin and its citations in the literature. However, due to the non-reversible covalent nature of the bond between the HHP and the anti-myosin S2 peptide, there was a concern that it may interfere with the anti-myosin S2 peptides function. The expense factor also being in mind, this led us

to think about a cheaper alternative that might be more readily available, and most importantly, has lower interference with the anti-myosin S2 peptides. The search was concluded with endorsing TA as a better alternative. It was shown in the literature that it could bind to GFP and several other proteins and deliver them to the heart. It was also shown that it required half an hour of shaking with other proteins to hook to it, however, it required 3 days of shaking with our peptides since the peptides are small. The TA-peptide bond was confirmed through mass spectroscopy. The samples were run in LC-MS system, but the TA clogged the column, so the run was switched into direct injection. The samples were run separately (peptides alone and TA alone) and together in water. The results were compared to runs in PBS with the same conditions. Only samples run together in PBS for 3 days or more showed consistent peaks that corresponded to the m/z value of the expected TA-anti-myosin S2 peptide, these peaks did not show in the TA alone or anti-myosin S2 peptides alone, thus they were assumed -with high confidence- that they were TA-anti-myosin S2 peptides peaks, except for one peak (581.5) which showed both in the DE alone and TA-DE runs. It was analyzed and determined to be DE peak when the DE was run by itself, and TA-DE peak when they were run together. According to our analysis, the bond appears to be an ester bond. This allows stable attachment in the blood and potential cleavage inside the cells by the esterase enzymes. The samples were prepared for mass spectroscopy runs by mixing TA and anti-myosin S2 peptides at 10:1 molarity ratio, however; due to the potential toxicity associated with the unbound TA, its concentration was dropped into half, and the peaks still showed in the spectrum. When the runs were lowered to equimolar concentrations, they were conspicuous more than before.

TA potential interference with anti-myosin S2 peptides functionality was tested using expansion microscopy and contractility assay. Expansion microscopy results showed the same pattern of binding to the myofibrils between the fluorescent TA-anti-myosin S2 peptides and the fluorescent anti-myosin S2 peptides alone. In both cases the destabilizer, which is specific to the S2 region, showed weaker staining at the C-zone; majorly due to the presence of the MyBPC in that area which is known to bind to the S2 and exclude the destabilizer, making the C-zone darker. In the stabilizer case the C-zone stained more intensely since it was able to bind to other parts of myosin without being limited to the S2. Along the same line, contractility assay showed that TA had minimum interference with the anti-myosin S2 peptides functions; the Kd did not vary much between the TA-ST compound and the stabilizer alone, neither did it vary between the TA-DE compound and the destabilizer alone. Even when the TA was tested by itself, it only affected contraction at 10 μM of TA or higher.

As for the TA-anti-myosin S2 peptides ability to internalize inside the myocytes, this feature was tested by another group of researchers. In their assay, the peptides were fluorescently tagged and allowed to interact with myocytes, 30 mins later the fluorescence was seen inside the cells. This provided a solid evidence that the peptides were able to enter inside the cells. The peptides were later tested for their ability to modify contractions of living myocytes, and surely the TA-DE increased contraction while the TA-ST decreased contraction.

Peptide based therapy is a very promising field since peptides are less toxic and more specific than small molecules, however; one of the major problems it faces is degradation by proteases in the blood. Several solutions were put forward to tackle this

issue, for example, cyclization of peptides and initiating them with Met, Ser, Ala, Thr, Val or Gly amino acids at the N-terminus makes them more resistant to degradation. Capping the N-terminus with methyl groups and the use of helical peptides are among other potential solutions. Other problems associated with peptide drugs are their expensive chemical synthesis, however, this can be solved by biological synthesis once a peptide shows a potential therapeutic effect. Another issue is the immunogenic reactions of the larger proteins, but these are less commonly used as drugs (Lee et al., 2019). Nonetheless, to address the above concerns and determine their efficiency and toxicity, the anti-myosin S2 peptides will undergo animal model tests. This will allow further edits to be introduced accordingly or allow progress to the next step.

6.2 Conclusion

This dissertation introduced novel peptides that may potentially have impact on patients who suffer from heart disease. These peptides modulate S2 instability by inducing a stabilizing effect through a potential therapeutic peptide called the stabilizer, which may have positive impact on FHCM patients, or they may induce a destabilizing effect through another potential therapeutic peptide called the destabilizer, which may impact DCM patients or patients who suffer from heart strokes. Their impact on S2 stability was determined using computational chemistry where the stabilizer increased the force required to unzip E930del myosin almost 9 times. While the destabilizer was shown to dimerize almost 3 times stronger to the myosin than the myosin dimerizing on itself. The peptides were then attached to TA to allow them to internalize into the heart muscle cells. The bond between TA and the anti-myosin S2 peptides was verified with mass spectroscopy. They are believed to bind with a covalent ester bond according to data

obtained from different runs. This type of bond is stable in the blood but is cleavable inside the cells by the esterases. The potential effect of TA on the peptides was then determined to be minimal through: expansion microscopy, which revealed that the peptides' pattern of binding to the sarcomere did not change with and without TA, and the contractility assay which showed that the Kd was similar for the peptides with and without TA. Together, this work prepared the peptides for the next level where they can be injected into animal models to determine their effect in vivo.

REFERENCES

Aboonasrshiraz, N. (2020). 'Impact of anti-S2 peptides on a variety of muscle myosin S2 isoforms and hypertrophic cardiomyopathy mutants revealed by fluorescence resonance energy transfer and gravitational force spectroscopy'. Doctoral dissertation. University of North Texas.

Acharyya, S., Villalta S., Bakkar, N., Bupha-Intr, T., Janssen, P., Carathers, M., Li ZW, Beg, A., Ghosh, S., Sahenk, Z., Weinstein, M., Gardner, K., Rafael-Fortney, J., Karin, M., Tidball, J., Baldwin, A. and Guttridge, D. (2007). 'Interplay of IKK/NF-kappaB signaling in macrophages and myofibers promotes muscle degeneration in Duchenne muscular dystrophy'*. J Clin Invest*. 2007;117:889–901.

Adhikari, A., Kooiker, K., Sarkar, S., Liu, C., Bernstein, D., Spudich, J. and Ruppel, K. (2016). Early-onset hypertrophic cardiomyopathy mutations significantly increase the velocity, force, and actin-activated ATPase activity of human beta-cardiac myosin. *Cell Rep* 17:2857–2864.

American Heart Association. (2020). Hypertrophic Cardiomyopathy. Viewed in June (2020). *https://www.heart.org/en/health-topics/cardiomyopathy/what-is-cardiomyopathy-in-adults/hypertrophic-cardiomyopathy.*

Alamo, L., Wriggers, W., Pinto, A., Bártoli, F., Salazar, L., Zhao, F.Q., Craig, R., and Padrón, R. (2008) Three-dimensional reconstruction of tarantula myosin filaments suggests how phosphorylation may regulate myosin activity. *J Mol Biol*. 384, 780-797.

Alcalai, R., Seidman, G. and Seidman, E. (2008) Genetic basis of hypertrophic cardiomyopathy: from bench to the clinics. *J Cardiovasc Electrophysiol*. 19(1):104-110

Al-Khayat, H. (2013). Three-dimensional structure of the human myosin thick filament: clinical implications. *Glob. Cardiol. Sci. Pract. 3*, 280-302.

Bader, D., Masaki, T. and Fischman, D. (1982). Immunochemical analysis of myosin heavy chain during avian myogenesis in vivo and in vitro. J.Cell Biol., 763-770.

Bang, L., Centner, T., Fornoff, F., Geach, J., Gotthardt, M., McNabb, M., Witt, C., Labeit, D., Gregorio, C., Granzier, H. and Labeit, S. (2001). 'The complete gene sequence of titin, expression of an unusual ~700 kDa titin isoform and its interaction with obscurin identify a novel Z-line to I-band linking system'. *Circulation Research* ;89:1065–1072

Baudenbacher, F., Schober, T., Pinto, J., Sidorov, V., Hilliard, F., Solaro, R., Potter, J., Knollmann, B. (2008) Myofilament ca2+ sensitization causes susceptibility to cardiac arrhythmia in mice. *J Clin Invest*. 118:3893–3903.

Betts, J., Desaix, P., Johnson, E., Johnson, J., Korol, O., Kruse, D., Poe, B., Wise, J., Womble, M., Young, K. (2017) Anatomy and Physiology open stax. P823-887. Rice University, Houston.

Blair, E., Redwood, C., Oliviera, M., Moolman-Smook, C., Brink, P., Corfield, V., Ostman-Smith, I. and Watkins, H. (2002). Mutations of the light meromyosin domain of the beta-myosin heavy chain rod in hypertrophic cardiomyopathy. *Circ Res*. 90(3):263-269.

Blankenfeldt, W., Thomä, H., Wray, J., Gautel, M. and Schlichting I. (2006). Crystal structures of human cardiac beta-myosin II S2-Delta provide insight into the functional role of the S2 subfragment. *Proc Natl Acad Sci U S A*. Nov 21;103(47):17713-7.

Burke, M., Himmelfarb, S., Harrington, W. 1973 Studies on the "hinge" region of myosin. Biochemistry.;12(4):701-10

Casella, F., Maack, J. and Lin, S. (1986) 'Purification and initial characterization of a protein from skeletal muscle that caps the barbed ends of actin filaments'. *J.Biol.Chem*. 261, 10915-10921.

Casella, F., Craig, W., Maack, D. and Brown, A**.** 1987 **'**Cap Z(36/32), a barbed end actin-capping protein, is a component of the Z-line of skeletal muscle'. J. *Cell Biol.,* 105 (1987), pp. 371-379.

Chen, F., Tillberg, P. and Boyden ,E. Optical imaging. Expansion microscopy. *Science*. 2015;347(6221):543-548.

Colegrave, M. and Peckham, M. (2014). Structural implications of β-cardiac myosin heavy chain mutations in human disease. *Anat Rec (Hoboken)*. 2014;297(9):1670-1680.

Coutu, P., Bennett, C., Favre, E., Day, S., Metzger, J. (2004). Parvalbumin corrects slowed relaxation in adult cardiac myocytes expressing hypertrophic cardiomyopathy-linked alpha-tropomyosin mutations. *Circ Res*. 94:1235–1241.

Ecken, J., Müller, M., Lehman, W., Manstein, J., Penczek, A. and Raunser, S. (2015). 'Structure of the F-actin-tropomyosin complex'. *Nature*. 519(7541):114-117.

Ehler, E., Gautel M. (2008). The sarcomere and sarcomerogenesis. *Adv Exp Med Biol*. 642:1-14.

Flashman, E., Watkins, H. and Redwood, C. (2007). Localization of the binding site of the C-terminal domain of cardiac myosin-binding protein-C on the myosin rod. *Biochem. J*. 401, 97-102.

Fu, L., Sun, X., Gao, Y., Chen, R. (2019). Tannic Acid: a Novel Calibrator for Facile and Accurate Mass Measurement of Electrospray Ionization Mass Spectrometry. J Am Soc Mass Spectrom. 30(8):1545-1549.

Frankel, A. and Pabo, C. (1988). 'Cellular uptake of the tat protein from human immunodeficiency virus'. *Cell*. 1988;55(6):1189-1193

Freiburg, A., Trombitas, K., Hell, W., Cazorla, O., Fougerousse, F., Centner, T., Kolmerer, B., Witt, C., Beckmann, S., Gregorio, C., Granzier, H. and Labeit, S. (2000). Series of exon-skipping events in the elastic spring region of titin as the structural basis for myofibrillar elastic diversity.*Circ. Res.* 86: 1114-1121

Freiburg, A. and Gautel, M. (1996). 'A molecular map of the interactions between titin and myosin-binding protein C. Implications for sarcomeric assembly in familial hypertrophic cardiomyopathy'. *Eur J Biochem*. 235(1-2):317-323.

Gautel, M. and Djinović-Carugo, K. (2016) 'The sarcomeric cytoskeleton: From molecules to motion', *Journal of Experimental Biology*, 219(2), pp. 135–145.

Gautel, M and Goulding, D. (1996). A molecular map of titin/connectin elasticity reveals two different mechanisms acting in series. *FEBS Lett*. 1996;385(1-2):11-14.

Green, E., Wakimoto, H., Anderson, R., Evanchik, M., Gorham, J., Harrison, B., Henze, M., Kawas, R., Oslob, J., Rodriguez, H., Song, Y., Wan, W., Leinwand, L., Spudich, J., McDowell, R., Seidman, J., Seidman, C. (2016). A small-molecule inhibitor of sarcomere contractility suppresses hypertrophic cardiomyopathy in mice. Science (New York, NY) 351:617–621.

Godfrey, J. and Harrington, W. (1970). Self-association in the myosin system at high ionic strength. I. Sensitivity of the interaction to pH and ionic environment. *Biochemistry*. 9(4):886-893.

Gokhin, D. and Fowler, V. (2013) A two-segment model for thin filament architecture in skeletal muscle. Nat Rev Mol Cell Biol 14:113– 119

Goodson, H. and Spudich J. (1993) Molecular evolution of the myosin family: Relationships derived from comparisons of amino acid sequences. *Proc Natl Acad Sci* USA **90**(2):659–663

Green, M. and Loewenstein, P. (1988). 'Autonomous functional domains of chemically synthesized human immunodeficiency virus tat trans-activator protein'. *Cell*. 1988;55(6):1179-1188.

Gundapaneni, D., and Root, D. (2005). High flexibility of the actomyosin crossbridge resides in skeletal muscle myosin subfragment-2 as demonstrated by a new single molecule assay. *J Struct Biol. 149*, 117-126

Harper, Q., Crawford, W., DelloRusso and C., Chamberlain, S. (2002). 'Spectrin-like repeats from dystrophin and alpha-actinin-2 are not functionally interchangeable. *Hum Mol Genet*. 11(16):1807-1815.

Hector, M., Rodriguez, S., Kawas, R., Song, Y., Sran, A., Oslob, J. (2015). Modulation of the cardiac sarcomere by a small molecule agent myk0000461: A potential therapeutic for the treatment of genetic hypertrophic cardiomyopathies. *Biophys J.* 106.

Henderson, C., Gomez, C., Novak, S., Mi-Mi, L., Gregorio, C. (2017). Overview of the Muscle Cytoskeleton. Compr Physiol. 18;7(3):891-944.

Herman, S., Lam, L., Taylor, R., Wang, L., Teekakirikul, P., Christodoulou, D., Conner, L., DePalma, R., McDonough, B., Sparks, E., Teodorescu, D., Cirino, A., Banner, N., Pennell, D., Graw, S., Merlo, Marco., Di Lenarda, A., Sinagra, G., Bos, J., Ackerman, M., Mitchell, R., Murry, C., Lakdawala, N., Ho, C., Barton, P., Cook, S., Mestroni, S., Seidman, J. and Seidman, C. (2012). 'Truncations of titin causing dilated cardiomyopathy'*. N. Engl. J. Med.* 16;366(7):619-28.

Homburger, J., Green, E., Caleshu, C., Sunitha, M., Taylor, R., Ruppel, K., Metpally, R., Colan, S., Michels, M., Day, S., Olivotto, L., Bustamante, C., Dewey, F., Ho, C., Spudich, J. and Ashley, E. (2016). 'Multidimensional structure-function relationships in human β-cardiac myosin from population-scale genetic variation'. *Proc Natl Acad Sci.* 113(24):6701-6706.

Hong, T., Shaw R. (2017). "Cardiac T-Tubule Microanatomy and Function." *Physiol Rev*. 97(1):227-252.

Huxley A.F., Simmons R.M. (1971). Proposed Mechanism of Force Generation in Striated Muscle*. Nature*. 233:533–538.

Kruger M, Wright J, Wang K. Nebulin as a length regulator of thin filaments of vertebrate skeletal muscles: Correlation of thin filament length, nebulin size, and epitope profile. J Cell Biol. 1991; 115:97–107.

Joshi, M., Yao, N., Myers, K. and Li, Z. (2013). 'Human serum albumin and p53-activating peptide fusion protein is able to promote apoptosis and deliver fatty acid-modified molecules'. *PLoS One*. 8(11):e80926.

Kampourakis, T., Yan, Z., Gautel, M., Sun, B. and Irving, M. (2014). 'Myosin binding protein-C activates thin filaments and inhibits thick filaments in heart muscle cells'. *Proc Natl Acad Sci* 111, 18763–8.

Kawana, M., Sarkar, S., Sutton, S., Ruppel, K. and Spudich, J. (2017). Biophysical properties of human β-cardiac myosin with converter mutations that cause hypertrophic cardiomyopathy. *Sci Adv* 3(2):e1601959.

Kulikovskaya, I., G. McClellan, J. Flavigny, L. Carrier, and S. Winegrad. (2003). Effect of MyBP-C binding to actin on contractility in heart muscle*. J. Gen. Physiol*. 122:761–774.

Kumar, A., Crawford, K., Close, L., Madison, M., Lorenz, J., Doetschman, T., Pawlowski, S., Duffy, J., Neumann, J., Robbins, J., Boivin, P., O'Toole, A. and Lessard L. (1997). 'Rescue of cardiac alpha-actin-deficient mice by enteric smooth muscle gamma-actin'. *Proc Natl Acad Sc*i ;94(9):4406–4411.

Labeit S et al (1991) Evidence that nebulin is a protein-ruler in muscle thin filaments. FEBS Lett 282:313–316.

Labeit, S. and Kolmerer, B. (1995). Titins: giant proteins in charge of muscle ultrastructure and elasticity. *Science*. 270(5234):293-296.

Lee, A., Harris, J., Khanna, K. and Hong, J. (2019). A Comprehensive Review on Current Advances in Peptide Drug Development and Design. *Int J Mol Sci*. 20(10):2383.

Lehman, W., Rosol, M., Tobacman, L. and Craig, R. (2001). Troponin organization on relaxed and activated thin filaments revealed by electron microscopy and three-dimensional reconstruction*. J. Mol. Biol.* 307:739–744

Leong, D., McMurray, J., Joseph, P., Yusuf, S. (2019). From ACE Inhibitors/ARBs to ARNIs in Coronary Artery Disease and Heart Failure (Part 2/5). *J Am Coll Cardiol*. 6;74(5):683-698.

Levine, R., Kensler, R., Yang Z., Stull J., Sweeney H. (1996). Myosin light chain phosphorylation affects the structure of rabbit skeletal muscle thick filaments. *Biophys J*. 71(2):898-907.

Li, Y., Brown, J.H., Reshetnikova, L., Blazsek, A., Farkas, L., Nyitray, L., and Cohen, C. (2003). Visualization of an unstable coiled coil from the scallop myosin rod. *Nature 424*, 341-345.

Linke, P., Clarkin, C., Di Leonardo, A., Tousa, A. and Wahl, M. (1996). 'A reversible, p53-dependent G0/G1 cell cycle arrest induced by ribonucleotide depletion in the absence of detectable DNA damage'. *Genes Dev* 10: 934–947.

Margossian, S., Lowey, S. (1982) Preparation of myosin and its subfragments from rabbit skeletal muscle. *Methods Enzymol*. 85 Pt B:55-71.

May, M., D'Acquisto, F., Madge, L., Glöckner, J., Pober, J. and Ghosh, S. (2000). "Selective inhibition of NF-kappaB activation by a peptide that blocks the interaction of NEMO with the IkappaB kinase complex". *Science*. 289(5484): 1550–4.

Mai, J., Mi, Z., Kim, S., Ng, B. and Robbins, P. (2001). A proapoptotic peptide for the treatment of solid tumors. *Cancer Res*. 61(21):7709-7712.

Mai, J., Shen, H., Watkins, S., Cheng, T. and Robbins, P. (2002). 'Efficiency of protein transduction is cell type-dependent and is enhanced by dextran sulfate'. *J Biol Chem*. 277(33):30208-30218.

Malik, F., Hartman, J., Elias, K., Morgan, B., Rodriguez, H., Brejc, K., Anderson, R., Sueoka, S., Lee, K., Finer, J., Sakowicz, R., Baliga, R., Cox, D., Garard, M., Godinez, G., Kawas, R., Kraynack, E., Lenzi, D., Lu, P., Muci, A., Niu, C., Qian, X., Pierce, D., Pokrovskii, M., Suehiro, I., Sylvester, S., Tochimoto, T., Valdez, C., Wang, W., Katori, T., Kass, D., Shen, Y., Vatner, S. and Morgans D. (2011). Cardiac myosin activation: a potential therapeutic approach for systolic heart failure. Science. 331:1439–43.

Margossian, S., Krueger, J., Sellers, J., Cuda, G., Caulfield, J., Norton, P., Slayter, H. Influence of the cardiac myosin hinge region on contractile activity. Proc Natl Acad Sci U S A. 88(11):4941-5.

Millevoi, S., Trombitas, K., Kolmerer, B., Kostin, S., Schaper, J., Pelin, K., Granzier, H., Labeit, S. (1998). Characterization of nebulette and nebulin and emerging concepts of their roles for vertebrate Z-discs. J Mol Biol. 11;282(1):111-23.

Messerli, F., Bangalore, S., Bavishi, C., Rimoldi, S. (2018). Angiotensin-Converting Enzyme Inhibitors in Hypertension: To Use or Not to Use? J Am Coll Cardiol;71(13):1474-1482.

Miyamoto, C., Fischman D. and Reinach, F. (1999) The interface between MyBP-C and myosin: site-directed mutagenesis of the CX myosin-binding domain of MyBP-C. *J Muscle Res Cell Motil* 20:703–715.

Moncman, C. and Wang, K. (2002) Targeted disruption of nebulette protein expression alters cardiac myofibril assembly and function. Exp Cell Res. 273:204–218.

Moss, L., Fitzsimons, P. and Ralphe, C. (2015). 'Cardiac MyBP-C regulates the rate and force of contraction in mammalian myocardium'. *Circ Res* 116, 183–92

Nag, S., Trivedi, V., Sarkar, S., Adhekari, A., Sunitha, M., Sutton, S., Ruppel, K., Spudich, J. The myosin mesa and the basis of hypercontractility caused by hypertrophic cardiomyopathy mutations. *Nat Struct Mol Biol*. 2017;24(6):525-533.

Nag, S., Sommese, R., Ujfalusi, Z., Combs, A., Langer, S., Sutton, S., Leinwand, L., Geeves, M., Ruppel, K. and Spudich J. (2015). Contractility parameters of human beta-cardiac myosin with the hypertrophic cardiomyopathy mutation R403Q show loss of motor function. *Sci Adv* 1:e1500511.

Pelin, K. & Wallgren-Pettersson, C. (2008). Nebulin—a giant chameleon. Adv Exp Med Biol 642:28–39

Peterson, J., Kline, W., Canan, B., Ricca, D., Kaspar, B., Delfín, D., DiRienzo, K., Clemens, P., Robbins, P., Baldwin, A., Flood, P., Kaumaya, P., Freitas, M., Kornegay, J., Mendell, J., Rafael-Fortney, J., Guttridge, D., and Janssen, P. (2011). 'Peptide-based inhibition of NF-κB rescues diaphragm muscle contractile dysfunction in a murine model of Duchenne muscular dystrophy'. *Mol Med*. 17(5-6):508-515.

Potter, J., Sheng, Z., Pan, B-S. and Zhao, J. (1995). 'A direct regulatory role for troponin T and dual role for troponin C in the Ca^{2+} regulation of muscle contraction.' *Journal of Biological Chemistry*. 270:2557–2562.

Purevjav, E., Varela, J., Morgado, M., Kearney, D., Li, H., Taylor, M., Arimura, T., Moncman, C., McKenna, W., Murphy, R., Labeit, S., Vatta, M., Bowles, N., Kimura, A., Boriek, A., Towbin, J. (2010). Nebulette mutations are associated with dilated cardiomyopathy and endocardial fibroelastosis. J Am Coll Cardiol. 56:1493–1502.

Rohde, J., Roopnarine, O., Thomas, D., Muretta, J. (2018). Mavacamten stabilizes an autoinhibited state of two-headed cardiac myosin. *Proc Natl Acad Sci USA.* 115: e7486-e7494.

Qadan, M., Migliore, J., Root, D. (2021). 'The Design of a Destabilizer Peptide to Disrupt SARS-CoV-2 Fusion with Its Targeted Cell Membrane'. *Biophysical Journal In press*.

Richard, P., Charron, P., Carrier, L., Ledeuil, C., Cheav, T., Pichereau, C., Benaiche, A., Isnard, R., Dubourg, O., Burban, M., Gueffet, J., Millaire, A., Desnos, M., Schwartz, K., Hainque, B. and Komajda, M. (2003) Hypertrophic cardiomyopathy: distribution of disease genes, spectrum of mutations, and implications for a molecular diagnosis strategy. *Circulation.* 107:2227–223210.1161/01.

Rethinasamy, P., Muthuchamy, M., Hewett, T., Boivin, G., Wolska, B., Evans, C., Solaro, R. and Wieczorek, D. (1998). Molecular and physiological effects of alpha-tropomyosin ablation in the mouse. *Circ Res*. 82(1):116-123.

Romani, A. and Maguire, M. (2002). Hormonal regulation of Mg^{2+} transport and homeostasis in eukaryotic cells. *Biometals.* 15:271–83

Root, D. (2002). The dance of actin and myosin: a structural and spectroscopic perspective. *Cell Biochem Biophys*. 37(2):111-139.

Root, D., and Reisler, E. (1992) Cooperativity of thiol-modified myosin filaments. ATPase and motility assays of myosin function. *Biophys. J. 63*, 730-740.

Root, D., Yadavalli, V, Forbes, J. and Wang, K. (2006). Coiled-coil nanomechanics and uncoiling and unfolding of the superhelix and alpha-helices of myosin. *Biophys J*.90(8):2852-2866.

Rybakova, N., Greaser, M., Moss, R. (2011). Myosin binding protein C interaction with actin: characterization and mapping of the binding site. *J Biol Chem*. 286(3):2008-2016.

Sanger, J., Wang, J., Fan, Y., White, J., Sanger, J. (2010) Assembly and dynamics of myofibrils. *J Biomed Biotechnol*.

Schwaiger, I., Sattler, C., Hostetter, D., Rief, M. (2002). The myosin coiled-coil is a truly elastic protein structure. Nat Mater.1(4):232-5

Seidman, E. (2000). 'Hypertophic cardiomyopathy: From man to mouse.' *J Clin Invest.* S9-13

Seidman, E. (2000). 'The genetic basis of hypertrophic cardiomyopathy'. *Cardiology Rounds*.4:1-6.

Singh, R., Dunn, J., Qadan, M., Hal,l N., Wang, K. Root, D. (2017). 'Whole length myosin binding protein C stabilizes myosin S2 as measured by gravitational force spectroscopy'. *Arch Biochem Biophys*. 638:41-51.

Singh, R. (2017). 'Stability of myosin subfragment-2 modulates the force produced by acto-myosin interaction of striated muscle'. *Doctoral dissertation*, University of North Texas

Shaffer, F., Kensler, W. and Harris, P. (2009). The myosin-binding protein C motif binds to F-actin in a phosphorylation-sensitive manner. *J. Biol. Chem*. 284:12318–12327.

Shin, M., Lee, H., Lee, M., Shin, Y., Song, J., Kang, S., Nam, D., Jeon, E., Cho, M., Do, M., Park, S., Lee, M., Jang, J., Cho, S., Kim, K. and Lee, H. (2018) 'Targeting protein and peptide therapeutics to the heart via tannic acid modification'. *Nat Biomed Eng*. (5):304-317.

Smith, P., Krohn, R., Hermanson, G., Mallia, A., Gartner, F., Provenzano, M., Fujimoto, E., Goeke, N., Olson, B. and Klenk D. (1985). Measurement of protein using bicinchoninic acid [published correction appears in Anal Biochem 1987 May 15;163(1):279]. *Anal Biochem*.150(1):76-85

Spudich, J. (2015). 'The myosin mesa and a possible unifying hypothesis for the molecular basis of human hypertrophic cardiomyopathy'. *Biochem Soc Trans*. 43(1):64-72.

Spudich, J., Aksel, T., Bartholomew, S., Nag, S., Kawana, M., Yu, C., Sarkar, S., Sung, J., Sommese , R., Sutton, S., Cho, C., Adhikari, A., Taylor, R., Liu, C., Trivedi, D. and Ruppel, K. (2016). 'Effects of hypertrophic and dilated cardiomyopathy mutations on power output by human β-cardiac myosin'. *J Exp Biol* ;219(Pt 2):161-167.

Squire, M., Luther, K. and Knupp, C. (2003). Structural evidence for the interaction of C-protein (MyBP-C) with actin and sequence identification of a possible actin-binding domain. *J Mol Biol.* 331:713–724.

Trivedi, V., Adhikari, S., Sarkar, S,, Ruppel, M. and Spudich, J. (2018). 'Hypertrophic cardiomyopathy and the myosin mesa: viewing an old disease in a new light'. *Biophys Rev*. 10:27–48

Toepfer C, Caorsi V, Kampourakis T, Sikkel, M., West, G., Leung, M-C., Al-Saud, S., MacLeod, K., Lyon, A., Marston, S., Sellers, J., Ferenczi, M. (2013). Myosin regulatory light chain (RLC) phosphorylation change as a modulator of cardiac muscle contraction in disease. *J Biol Chem*. 288(19):13446-13454.

Tonino, P., Pappas, C., Hudson, B., Labeit, S., Gregorio, C. and Granzier, H. (2010). Reduced myofbrillar connectivity and increased Z-disk width in nebulin-defcient skeletal muscle. J Cell Sci 123:384– 391

Waldmüller, S., Sakthivel, S., Saadi, A., Selignow, C., Rakesh, P., Golubenko, M., et al. . (2003). Novel deletions in MYH7 and MYBPC3 identified in Indian families with familial hypertrophic cardiomyopathy. *J. Mol. Cell. Cardiol*. 35, 623–636.

Walsh, R., Buchan, R., Wilk, A., John, S., Felkin, L., Thomson, K., Hak Chiaw, T., Loong, K., Pua, C., Raphael, C., Prasad, S., Barton, P., Funke, B., Watkins, H., Ware, J. and Cook, S. (2017). Defining the genetic architecture of hypertrophic cardiomyopathy: re-evaluating the role of non-sarcomeric genes. *Eur Heart J*. 38(46):3461-3468.

Wender, P., Mitchell, D., Pattabiraman, K., Pelkey, E., Steinman, L. and Rothbard, J. (2000). 'The design, synthesis, and evaluation of molecules that enable or enhance cellular uptake: peptoid molecular transporters'. *Proc Natl Acad Sci* ;97(24):13003-13008.

Win, K., Teng, C., Jin, M., Ye, E., Tansil, N. and Han, M. (2012). 'On-site chemical reaction lights up protein assemblies in cells'. *Analyst*. 137(10):2328-2332.

Witt, C., Burkart, C., Labeit, D., McNabb, M., Wu, Y., Granzier, H. and Labeit, S. (2006). Nebulin regulates thin filament length, contractility, and Z-disk structure in vivo. *EMBO J* 25:3843–3855.

Yuen, M., Ottenheijm, C. Nebulin: big protein with big responsibilities. J Muscle Res Cell Motil. 2020 Mar;41(1):103-124.

Xia, S., Zhu, Y., Liu, M., Lan, Q., Xu, W., Wu, Y., et al. (2020). 'Fusion mechanism of 2019-nCoV and fusion inhibitors targeting HR1 domain in spike protein'. *Cell. Mol. Immunol.* 17, 765–767.

Zahid, M. and Robbins P. (2011).' Identification and characterization of tissue-specific protein transduction domains using peptide phage display'. *Methods Mol. Biol.* ;683:277–289

Zhao, Y., Bucur, O., Irshad, H., Chen, F., Weins, A., Stancu, A., Oh, E., DiStasio, M., Torous, V., Glass, B., Stillman, I., Schnitt, S., Beck., A. and & Boyden E. (2017). 'Nanoscale imaging of clinical specimens using pathology-optimized expansion microscopy '. *Nature Biotechnology*. 35(8):757-764.